e-ISSN: 3023-6487

JRM

Journal of Radiology in Medicine

Volume: 1

Issue: 3

Year: 2024

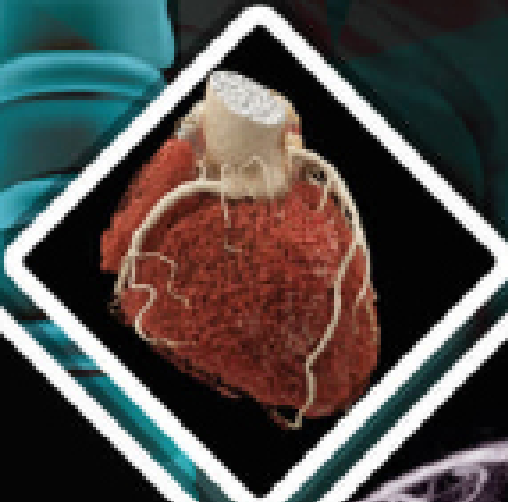

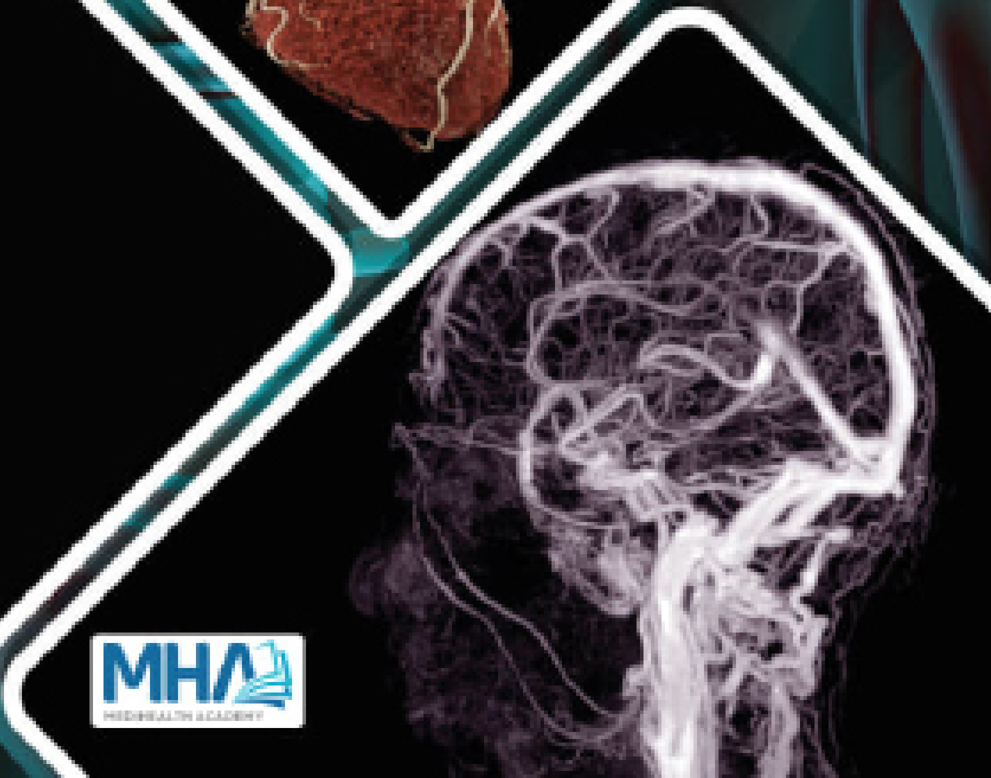

MHA
MEDIHEALTH ACADEMY

Journal of Radiology in Medicine

Contents

Volume: 1 Issue: 3 Year: 2024

ORIGINAL ARTICLES

Morphometric comparison of ruptured and non-ruptured intracranial aneurysms....37-41
Duman E, Özen Ö, Kesim Ç, Yıldırım E.

Results and complications of percutaneous co-axial trans-thoracic biopsy in lung masses: our clinical experience....42-45
Özdemir A, Şahan MH.

Evaluation of hip angles with magnetic resonance imaging in early stage femoral head osteonecrosis....46-49
Şahan MH, Mete D.

Evaluation of stress levels in adult patients waiting for ultrasonography examination in radiology unit....50-53
Bekin Sarıkaya PZ, Tekeli Kunt A, Çolakoğlu G, et al.

CASE REPORT

Brain abscess mimicking an intracranial mass on radiologic examinations: a case report 54-57
Sevimoğlu Ö, Erdoğan AM, Özdemir A, et al.

Journal of
Radiology in Medicine

Original Article

Doi: 10.51271/JRM-0011

Morphometric comparison of ruptured and non-ruptured intracranial aneurysms

Enes Duman[1], Özgür Özen[2], Çağrı Kesim[3], Erkan Yıldırım[3]

[1]*Department of Radiology, Vocational School of Health Services, Faculty of Medicine, Antalya Science University, Antalya, Turkiye*
[2]*Division of Interventional Radiology, Department of Radiology, Faculty of Medicine, Başkent University, Ankara, Turkiye*
[3]*Department of Radiology, Konya Hospital, Interventional Radiology Section, Faculty of Medicine, Başkent University, Konya, Turkiye*

Received: 02.06.2024 ◆ **Accepted**: 17.07.2024 ◆ **Published**: 29.07.2024

Cite this article: Duman E, Özen Ö, Kesim Ç, Yıldırım E. Morphometric comparison of ruptured and non-ruptured intracranial aneurysms. *J Radiol Med.* 2024;1(3):37-41.

Corresponding Author:Çağrı Kesim, cagrikesim@hotmail.com

ABSTRACT

Aims: Morphologic features of cerebral aneurysms that may be related to the rupture of a cerebral aneurysm. We used precise measurements and software to create a comprehensive data set and determine the parameters that may affect cerebral aneurysm rupture risk.

Methods: After excluding patients with vasospasm, late admission (later than 72 hours), and previous hemorrhage or treatment history, 95 consecutive patients with 112 cerebral aneurysms were included in the study. Ten morphological parameters of aneurysms were compared between ruptured and non-ruptured aneurysms. These parameters include the size, depth and neck size of the aneurysm, the diameter of the parent artery and their ratio to each other.

Results: There were 87 ruptured and 25 non-ruptured cerebral aneurysms. The mean size, d90, dmax, SR1, SR2, and AR1 parameters of the ruptured cerebral aneurysms were significantly higher than the non-ruptured aneurysms, and SR1 was the strongest parameter for determining aneurysm rupture risk, which is the ratio of the maximum depth of the aneurysm to the average size of the parent vessel. Nevertheless, there was no significant correlation between age, sex, and aneurysm location.

Conclusions*:* It is observed that the perpendicular (d90) and maximum depth (dmax) of the aneurysm and the ratios of including these elements are greater in ruptured aneurysms. These results suggest that the depth of an aneurysm is probably the most relevant factor to the risk of rupture.

Keywords*:* Aspect ratio; cerebral aneurysm; cerebral hemorrhage; ruptured aneurysms; rupture risk; size ratio

INTRODUCTION

Aneurysmal subarachnoid hemorrhage (a-SAH) has a high morbidity and mortality, whereas non-aneurysmal subarachnoid hemorrhage (n-SAH) has a better prognosis. Therefore, diagnosis and treatment of an aneurysm should be done before rupture.[1] There are some prognostic factors such as size, location, and multiplicity for the risk of rupture.[2] Certain risk factors have been associated with an aneurysm and its rupture. Many studies have reported that the risk of aneurysm rupture is 1-2% per year.[3] Some previous studies have shown that some factors increase the risk of aneurysm rupture, such as genetic predisposition, female gender, connective tissue disease, the growth rate of aneurysm and PHASES score, and the presence of multiple cerebral aneurysms.[4,5]

Some morphological parameters have been studied in relation to the risk of aneurysm rupture, and morphological studies have been associated with aneurysm shape, parent vessel size, and depth. Each method provides insight and important data on aneurysm growth, rupture, and potential regrowth. Some morphologic parameters have been reported in the literature, but measurements of these parameters have been calculated differently, and different parameters have been evaluated in various studies.[6-12] Appropriate parameters that characterize the geometry of the intracranial aneurysm can capture the characteristic hemodynamics and potentially predict the risk of rupture. Several previous studies have investigated such parameters.

The most used parameter is the size of the intracranial aneurysm. Although aneurysms larger than 10 mm are considered prone to bleeding, several studies have shown that a large percentage of ruptured aneurysms are smaller than ten millimeters.[13] The relationship between intracranial aneurysm rupture risk and intracranial aneurysm size has not been fully understood. The aneurysm's shape has also been studied, and certain shape parameters show a stronger correlation with rupture than intracranial aneurysm size. Aspect ratio (AR), defined as intracranial aneurysm height divided by neck diameter, is the most studied shape parameter. Although most results confirm the importance of AR, there is no common threshold in the literature. Other, more sophisticated shape parameters such as the undulation index, nonsphere index, and ellipticity index have been proposed to account for the three-dimensionality (3D) of the intracranial aneurysm.[13] 3D parameters promise better predictions than lower-dimensional parameters such as size or AR and are further investigated in the current study.

This study includes all parameters used in the various papers in the literature. Our aim was to find the strongest morphometric parameters for rupture risk by evaluating all parameters from the literature. We also investigated statistically significant associations between aneurysm rupture and other parameters such as age, sex, and location of the aneurysm.

METHODS

This is a retrospective observational single-center study. The study was carried out with the permission of the Başkent University Faculty of Medicine Ethics Committee (Date: 26.06.2024, Decision No: KA24/238). All procedures performed in studies involving human participants were in accordance with the ethical standards of the institutional research committee and with the 1964 Helsinki Declaration and its later amendments or comparable ethical standards.

Patient Selection

Patients with vasospasm, late admission (later than 72 hours), and previous SAH or treatment history were excluded from the study. Except for these conditions, ninety-five consecutive patients who underwent cerebral digital subtraction angiography (DSA) (Artis Zee, Siemens, Germany) between 2012 and 2015 and had a cerebral aneurysm were included. The angiographic images and electronic medical records of the patients were scanned.

Imaging Technique

For cerebral DSA, a total of 10-12 ml of nonionic contrast agent (Optiray 300, Mallinckrodt Health, İstanbul, Türkiye) was injected from each internal carotid artery and vertebral arteries at a rate of 5 ml/second using an automated injection device (Liebel-Flarsheim, Angiomat Illumena, Cincinnati/USA). For 3D angiography, 35 ml of nonionic contrast agent was injected from the right or left carotid artery at a 5 ml/second rate with an automatic power injector. After the one-second delay and seven-second rotation duration, 3D images were obtained with Siemens DSA suit's version VB20/VB21 software.

Data Collection

Measurements were performed by two radiologists using the 3D angiography images. They reviewed the images together and reached consensus on the measurements. All angiographies in the SAH group were obtained within 12 hours of SAH. Ten morphological parameters were sought, all calculated by the 3D software of the DSA unit.

Morphometric Parameters

Size: If the aneurysms' shapes were regular (not lobulated), we used the maximum perpendicular height from the neck of the aneurysm or the axial diameter. For irregular and lobulated aneurysms, we used the arithmetic mean of the smallest and largest diameters of the aneurysm.

Depth (d_{90}, d_{max}): We used two different calculations for depth; d90 (Figure 1, black arrow): the maximum perpendicular distance from the center of the neck to any point on the aneurysm wall, dmax (Figure 1, white arrow): the maximum distance between the dome of the aneurysm and the center of the neck.

Figure 1. Volume rendering technique image of a ruptured right middle cerebral artery bifurcation aneurysm. * The lengths d90 and dmax are indicated by black and white arrows, respectively

Neck size (n): Neck size represents the largest axial diameter at the aneurysm orifice.

Size of the parent vessel (p): If the aneurysm was on the lateral side of the wall, we used only the size of the parent vessel from which the aneurysm originated. We used the arithmetic mean of the parent vessels' size if the aneurysm was located at a bifurcation (Figure 2).

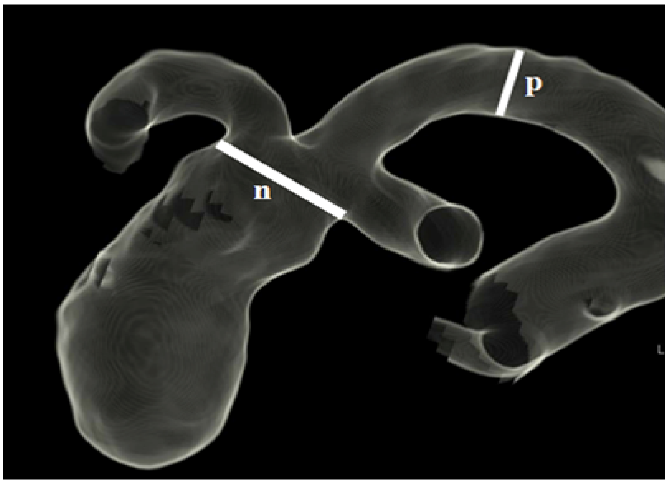

Figure 2. Volume Rendering Technique image of a ruptured right middle cerebral artery bifurcation aneurysm. *"Neck size" (n) and "size of the parent vessel" (p) are shewed

Aspect ratio (AR): AR1 was defined as the ratio of the maximum depth to the width of the aneurysm neck. AR2 was the perpendicular depth ratio to the aneurysm neck's width. AR1=dmax/n, AR2=d90/n.

Size ratio (SR): SR1 was calculated by dividing the maximum depth of the aneurysm by the average parent vessel size. SR2 was calculated by dividing the perpendicular depth of the aneurysm by the average parent vessel size. SR1=dmax/p, SR2=d90/p.

Ostium ratio (OR): OR was described as the ratio of the width of the aneurysm neck to the parent vessel size. OR=n/p.

Statistical Analysis

Two independent groups of ruptured and non-ruptured patients were compared using a T-test for normally distributed parameters. Mann-whitney U test was used for non-normally distributed parameters. Crosstab analysis with a chi-square test was used to determine the correlation between categorical parameters and the presence of rupture. Logistic regression models were sought and developed to predict rupture risk as a function of morphologic parameters. Logistic regression was used to evaluate the predictive value of rupture probability based on those independent parameters that differed significantly between ruptured and non-ruptured aneurysms. The logistic regression models were searched and developed in our study to predict the risk of rupture depending on the morphologic parameters.

RESULTS

Cerebral DSA was performed in 95 patients, with a total aneurysms of 112. Thirty-seven patients (40.2%) were male and had 35 ruptured cerebral aneurysms; 58 patients (59.8%) were female and had 52 ruptured cerebral aneurysms. There were 87 ruptured and 25 non-ruptured cerebral aneurysms. The mean age in the first group with a ruptured aneurysm was 56.6±11.04 years, and in the other group, 56.3±10.49 years. There was no statistically significant association between sex (Table 1), age, and rupture (Table 2).

Forty-two aneurysms (37.5%) were located at the anterior communicating artery (A-com), and 36 of them were ruptured (41.4%); 27 aneurysms (24.1%) were located at the middle cerebral artery (MCA) bifurcation, and 23 of them were ruptured (26.4%); 24 aneurysms (21.4%) were located at the internal carotid artery (ICA), and 14 of them were ruptured (16.1%); 11 aneurysms (9.8%) were located at the posterior communicating artery (P-com), and 8 of them were ruptured (9.2%); one aneurysm was located at the posterior cerebral artery (PCA), and it was unruptured (0.9%); five aneurysms (4.5%) were located at the basilar artery (BA), 4 of them were ruptured (4.6%); two aneurysms (1.8%) were located at the posterior inferior cerebellar artery (PICA), and both aneurysms were ruptured (1.8%). The most common aneurysm site was the A-com, followed by the MCA bifurcation. The most common non-ruptured aneurysm site was the ICA and then the A-com. The most common site of ruptured aneurysms was the A-com and then MCA.The morphological parameters of the ruptured aneurysms, such as size, d90, dmax, SR1, SR2, and AR1, were significantly different from those of the non-ruptured aneurysms. The mean size of the ruptured cerebral aneurysms was significantly larger (7.4±4.54 mm) compared with that of the non-ruptured aneurysms (4.92±3.06 mm) ($p<0.001$). Mean d90 was 6.55±3.81 mm in ruptured aneurysms and 3.81±1.6 mm in non-ruptured aneurysms ($p<0.001$).

The mean dmax value was 7.78±4.16 mm in ruptured aneurysms, and in non-ruptured aneurysms, 4,58±1.81 mm ($p<0.001$). Mean SR1 was 3.06±1.56 in ruptured aneurysms and 1.67±0.82 in non-ruptured aneurysms ($p<0.001$). Mean SR2 was 2.64±1.43 in ruptured aneurysms and 1.51±0.76 in non-ruptured aneurysms ($p<0.001$). In ruptured aneurysms, the mean AR1 value was 2.37±1.12; in non-ruptured aneurysms, 1.77±1.19 ($p=0.001$) (Table 2). Logistic regression was used to assess the independent predictive value of those parameters that differed significantly between ruptured and non-ruptured aneurysms (Table 3). In the final model, only SR1 remained, the most significant morphological predictive parameter for rupture (Table 3, Model 1.1). The risk of rupture of the aneurysm whose value of SR1 was known can be determined using a logistic regression model (Table 3, Model 1.2). Linear regression model 1.2 showed us the extent to which a change in SR1 value increases or decreases the probability of rupture of the intracranial aneurysm.

Table 1. Chi-Square analysis for rupture and sex

	RUPTURE					
	YES		NO		TOTAL	
SEX	Count	%Within rupture	Count	%Within Rupture	Count	%Within Rupture
MALE	35	40.2%	10	40%	45	40.2%
FEMALE	52	59.8%	15	60%	67	59.8%
TOTAL	87	100%	25	100%	112	100

Chi-square = 0.000, p=0.984

Table 2. Comparison of the parameters according to the groups.

	RUPTURE STATUS							
	YES			NO				
	N	Mean	Std. Deviation	N	Mean	Std. Deviation	TEST	Sig.
Age	87	56.6	11.04	25	56.3	10.49	t=-0.144	0.885
p	87	2.7138	0.8407	25	2.9	0.94296	t=0.95	0.344
n	87	3.323	1.24178	25	2.992	0.84504	t=-1.25	0.214
d90	87	6.5598	3.81312	25	3.8104	1.60573	t=-5.289	<0.001*
dmax	87	7.7885	4.16272	25	4.584	1.81675	t=-5.568	<0.001*
OR	87	1.3247	0.61757	25	1.124	0.47459	z=-1.654	0.098
SR2	87	2.6408	1.43862	25	1.51	0.76676	t=-5.199	<0.001*
AR2	87	2.0736	0.76272	25	1.748	0.66965	t=-1.93	0.056
SR1	87	3.0655	1.56293	25	1.676	0.82173	t=-5.92	<0.001*
AR1	87	2.377	1.12629	25	1.776	1.19906	z=-3.451	0.001*

p: size of the parent vessel (mm)
n: neck size (mm)
d90 and dmax: maximum and perpendicular depth of aneurysm (mm)
OR(n/p): ostium ratio (mm/mm)
AR1(dmax/n) and AR2(d90/n): aspect ratio (mm/mm)
SR1(dmax/p) and SR2(d90/p): size ratio (mm/mm)

Table 3. Logistic regression models of the aneurysms' morphologic parameters

MODEL 1. 1	B	S.E.	Wald	df	Sig.	Exp(B)	The correct classification ratio of the patient group (%)	The correct classification ratio of the control group (%)	General right classification ratio (%)
p	.545	.701	.605	1	.437	1.725	(83/87) = 95.4	(10/25) = 40.0	(93/112) = 83.0
n	-.353	.493	.514	1	.473	.702			
d90	.121	.575	.044	1	.833	1.129			
dmax	.396	.384	1.064	1	.302	1.486			
OR	-.788	1.068	.544	1	.461	.455			
SR_2	.716	1.341	.285	1	.594	2.046			
AR_2	-.731	.564	1.680	1	.195	.481			
SR_1	1.249	.890	1.967	1	.161	3.486			
AR_1	-.473	.460	1.057	1	.304	.623			
Size	-.271	.182	2.220	1	.136	.763			
Constant	-1.301	2.373	.300	1	.584	.272			
MODEL 1.2 FINAL MODEL									
SR_1	1.072	.276	15.108	1	.000	2.920	(83/87) = 95.4	(8/25) = 32.0	(91/112) = 81.3
Model 2									
d_{90}	.416	.125	11.111	1	.001	1.516	(83/87) = 95.4	(2/25) = 8.0	(85/112) = 75.9
Model 3									
d_{max}	.432	.122	12.490	1	.000	1.541	(83/87) = 95.4	(4/25) = 16.0	(87/112) = 77.7
Model 4									
SR_2	.984	.273	12.987	1	.000	2,674	(81/87) = 93,1	(3/25) = 12,0	(84/112) = 75.0
Model 5									
AR_1	.683	.302	5.120	1	.024	1.980	(87/87) = 100.0	(0/25) = 0.0	(87/112) = 77.7

p: size of the parent vessel (mm)
n: neck size (mm)
d90 and dmax: maximum and perpendicular depth of aneurysm (mm)
OR(n/p): ostium ratio (mm/mm)
AR1(dmax/n) and AR2(d90/n): aspect ratio (mm/mm)
SR1(dmax/p) and SR2(d90/p): size ratio (mm/mm)

DISCUSSION

Based on the results of two different recent meta-analyses on a population of 50 subjects, 33% male and 67% female, with a mean age of 50 years, without comorbidities, the incidence of cerebral aneurysms was reported to be 2%, and the annual probability of rupture 1.9%. From these results, we can infer that most cerebral aneurysms do not rupture.[14,15] The PHASES (population, hypertension, age, size of aneurysm, previous SAH from another aneurysm, location of aneurysm) score is a model that indicates the absolute risk of aneurysm rupture.[16] The aneurysm rupture risk increases when the PHASES score is high.[5]

We found that the mean size of ruptured cerebral aneurysms was significantly larger (7.4±4.54 mm) than that of non-ruptured aneurysms (4.92±3.06 mm). Indeed, many studies have reported that size is an important parameter for rupture, although the actual range for rupture risk is controversial.[17] However, most cases of a-SAH are due to small aneurysms in the anterior circulation,[18,19] so the size of aneurysm alone is not sufficient to assess rupture risk.

The aneurysm location is associated with the rupture status. Most clinical series reported that ruptured aneurysms were frequently located on the A-com, and the non-ruptured aneurysms were frequently located on the MCA, as found in the autopsy series. [17,20] Beck et al.[20] reported in their study of 155 aneurysms that ruptured aneurysms were more frequently located on the A-com than non-ruptured aneurysms. Similar to the literature, the most common aneurysm site and the most common rupture site in our study were A-com. In contrast to the autopsy series in the literature, the internal carotid artery is the most common site for non-ruptured aneurysms.

Several morphological parameters, including AR, SR, and OR, have been associated with cerebral aneurysm rupture.[6-8,11,12] SR is the most important calculation for predicting the rupture risk of these parameters. For example, in our serie, when the SR1 value is 1.3, the risk of rupture according to our model is 55.7%; when the SR1 value is 4, it increases to 95.7%, explaining that this increase in the SR1 value increases the risk of rupture by 40%. Dhar et al.[8] reported that AR and SR were significantly correlated with rupture. Their study included 45 aneurysms (25 non-ruptured, 20 ruptured). Ma D et al.[12] reported that SR and AR were associated with rupture. SR showed a more significant association with ruptured aneurysms than AR. Cai W et al.[7] studied AR and SR and reported that only SR could be a decisive factor correlating with aneurysm rupture. Nikolic I et al.[10] reported that OR and AR were statistically significant parameters for predisposition to rupture of intracranial aneurysms. However, they did not calculate SR in their study.

The values of SR1, SR2, and AR1 were significantly different between ruptured and non-ruptured aneurysms. These parameters were higher in ruptured aneurysms. Logistic regression was used to evaluate the independent predictive value of the parameters that differed significantly between ruptured and non-ruptured aneurysms, and only SR1 remained in the final model, which was the most significant morphological predictive parameter for rupture. OR, size, parent artery size, AR2, and neck size were not associated with rupture.

Limitations

The major limitation of this study is that the measurement of the aneurysms was performed after rupture, and the morphology of an aneurysm changes after rupture.[21] It is generally accepted that vasospasm affects the geometry of the truncal artery of the cerebral aneurysm approximately five days after hemorrhage.[9] In particular, the logistic regression data are misleading because if we want to predict the probability of rupture, we need to assess a non-ruptured aneurysm, and the model cannot be generalized to non-ruptured aneurysms. The best study design is to conduct a prospective study in a group of patients with nonruptured aneurysms and follow them up, but this is not feasible and ethical because patients diagnosed with cerebral aneurysm should be treated to prevent rupture of an aneurysm. Most of our patients underwent angiography within 24 hours of the first hemorrhage. Therefore, vasospasm is not expected in our patients, but some who had a quiet clinic may have contacted emergency services later. Apart from these, another study limitation is the small number of patients in the control group.

CONCLUSION

Increased size, d90, dmax, SR1, SR2, and AR1 were significantly associated with ruptured aneurysms. We can say that they are all predictive parameters for aneurysm behavior, and among them, SR1 is the strongest parameter for determining aneurysm rupture risk. These results show that the perpendicular and especially the maximum depth of an aneurysm is probably the factor that most influences the risk of aneurysm rupture. Compared to the maximum depth of the aneurysm, the perpendicular depth or its neck size seems less associated with the risk of rupture.

ETHICAL DECLARATIONS

Ethics Committee Approval

The study was carried out with the permission of the Başkent University Faculty of Medicine Ethics Committee (Date: 26.06.2024, Decision No: KA24/238).

Informed Consent

Because the study was designed retrospectively, no written informed consent form was obtained from patients.

Referee Evaluation Process

Externally peer-reviewed.

Conflict of Interest Statement

The authors have no conflicts of interest to declare.

Financial Disclosure

The authors declared that this study has received no financial support.

Author Contributions

All of the authors declare that they have all participated in the design, execution, and analysis of the paper, and that they have approved the final version.

REFERENCES

1. Jung JY, Kim YB, Lee JW, Huh SK, Lee KC. Spontaneous subarachnoid haemorrhage with negative initial angiography: a review of 143 cases. *J Clin Neurosci.2006;13(10):1011-1017. doi:10.1016/j.jocn.2005.09.007*
2. International Study of Unruptured Intracranial Aneurysms I. Unruptured intracranial aneurysms--risk of rupture and risks of surgical intervention. *N Engl J Med*. 1998;339(24):1725-1733.
3. Juvela S, Poussa K, Lehto H, Porras M. Natural history of unruptured intracranial aneurysms: a long-term follow-up study. *Stroke*. 2013;44 (9): 2414-2421.. doi:10.1161/STROKEAHA.113.001838
4. Juvela S. Risk factors for multiple intracranial aneurysms. *Stroke*. 2000;31(2):392-397. doi:10.1161/01.str.31.2.392
5. Backes D, Vergouwen MD, Tiel Groenestege AT, et al. PHASES score for prediction of intracranial aneurysm growth. *Stroke*. 2015;46(5):1221-1226. doi:10.1161/STROKEAHA.114.008198
6. Tykocki T, Kostkiewicz B. Aneurysms of the anterior and posterior cerebral circulation: comparison of the morphometric features. *Acta Neurochir*. 2014;156(9):1647-1654. doi:10.1007/s00701-014-2173-y
7. Cai W, Shi D, Gong J, et al. Aremorphologic parameters actually correlated with the rupture status of anterior communicating artery aneurysms? *World Neurosurg*. 2015;84(5):1278-1283. doi:10.1016/j.wneu.2015.05.060
8. Dhar S, Tremmel M, Mocco J, et al. Morphology parameters for intracranial aneurysm rupture risk assessment. *Neurosurgery*. 2008;63(2):185-196; discussion 196-197. doi:10.1227/01.NEU.0000316847.64140.81
9. Morgan M, Halcrow S, Sorby W, Grinnell V. Outcome of aneurysmal subarachnoid haemorrhage following the introduction of papaverine angioplasty. *J Clin Neurosci*. 1996;3(2):139-142. doi:10.1016/s0967-5868(96)90007-7
10. Nikolic I, Tasic G, Bogosavljevic V, et al. Predictable morphometric parameters for rupture of intracranial aneurysms - a series of 142 operated aneurysms. *Turk Neurosurg*. 2012;22(4):420-426. doi:10.5137/1019-5149.JTN.4698-11.1
11. Rahman M, Smietana J, Hauck E, et al. Size ratio correlates with intracranial aneurysm rupture status: a prospective study. *Stroke*. 2010;41(5):916-920. doi:10.1161/STROKEAHA.109.574244
12. Ma D, Tremmel M, Paluch RA, Levy EI, Meng H, Mocco J. Size ratio for clinical assessment of intracranial aneurysm rupture risk. *Neurol Res*. 2010;32(5):482-486. doi:10.1179/016164109X12581096796558
13. Raghavan ML, Ma B, Harbaugh RE. Quantified aneurysm shape and rupture risk. *J Neurosurg*. 2005;102(2):355-362. doi:10.3171/jns. 2005.102.2.0355
14. Rinkel GJ, Djibuti M, Algra A, van Gijn J. Prevalence and risk of rupture of intracranial aneurysms: a systematic review. *Stroke*. 1998;29(1):251-256. doi:10.1161/01.str.29.1.251
15. Vlak MH, Algra A, Brandenburg R, Rinkel GJ. Prevalence of unruptured intracranial aneurysms, with emphasis on sex, age, comorbidity, country, and time period: a systematic review and meta-analysis. *Lancet Neurol*. 2011;10(7):626-636. doi:10.1016/S1474-4422(11)70109-0
16. Greving JP, Wermer MJ, Brown RD, Jr., et al. Development of the PHASES score for prediction of risk of rupture of intracranial aneurysms: a pooled analysis of six prospective cohort studies. *Lancet Neurol*. 2014;13(1):59-66. doi:10.1016/S1474-4422(13)70263-1
17. Asari S, Ohmoto T. Natural history and risk factors of unruptured cerebral aneurysms. *Clin Neurol Neurosurg*. 1993;95(3):205-214. doi: 10.1016/0303-8467(93)90125-z
18. Forget TR, Jr., Benitez R, Veznedaroglu E, et al. A review of size and location of ruptured intracranial aneurysms. *Neurosurgery*. 2001;49(6):1322-1325.
19. Weir B, Disney L, Karrison T. Sizes of ruptured and unruptured aneurysms in relation to their sites and the ages of patients. *J Neurosurg*. 2002;96(1):64-70. doi:10.3171/jns.2002.96.1.0064
20. Beck J, Rohde S, el Beltagy M, et al. Difference in configuration of ruptured and unruptured intracranial aneurysms determined by biplanar digital subtraction angiography. *Acta Neurochir (Wien)*. 2003;145(10):861-865.
21. Skodvin TO, Johnsen LH, Gjertsen O, Isaksen JG, Sorteberg A. Cerebral aneurysm morphology before and after rupture: nationwide case series of 29 aneurysms. *Stroke*. 2017;48(4):880-886.

Journal of Radiology in Medicine

Original Article

Doi: 10.51271/JRM-0012

Results and complications of percutaneous co-axial trans-thoracic biopsy in lung masses: our clinical experience

Adnan Özdemir[1], Mehmet Hamdi Şahan[2]

[1]Department of Radiology, Faculty of Medicine, Kırıkkale University, Kırıkkale, Turkiye
[2]Department of Radiology, Faculty of Medicine, Gaziantep University, Gaziantep, Turkiye

Received: 27.06.2024 ◆ **Accepted**: 20.07.2024 ◆ **Published**: 29.07.2024

Cite this article: Özdemir A, Şahan MH. Results and complications of percutaneous co-axial trans-thoracic biopsy in lung masses: our clinical experience . J Radiol Med. 2024;1(3):42-45.

Corresponding Author: Adnan Özdemir , dradnanozdemir@gmail.com

ABSTRACT

Aims: The aim of our study was to evaluate the diagnostic rates and procedure-related complications in lung masses undergoing computed tomography (CT)-guided percutaneous coaxial trans-thoracic biopsy (PCTTB).
Methods: We retrospectively analyzed 117 patients who underwent CT-guided PCTTB between January 2016 and December 2018. A 64 slice Multislice-CT was used in each patient. A core biopsy was performed with a 16–18-gauge needle using the co-axial method. The demographic characteristics of the patients, post-procedural diagnosis rates, and complications were evaluated.
Results: Of 117 patients, 93 were male (mean age 67.9±10.8 years) and 24 were female (mean age 64.2±15.2 years). The pathologic evaluation of three patients was reported as "insufficient material". The diagnostic sensitivity of CT-guided PCTTB was 97.4%. Malignant lesions were detected in 70 patients (59.8%) and benign lesions in 44 patients (37.9%). The most common complication was pneumothorax, which occurred in 24 (20.5%) patients. A thoracic tube was inserted in three of these patients, while the others were discharged with follow-up. Other complications were hemorrhage (10.3%) and hemoptysis (12%), respectively. While mortality in CT-guided biopsy was associated with air embolization in some studies, mortality was not present in our study.
Conclusion: CT-guided PCTTB lung biopsies have a high diagnostic rate and acceptable complications. Percutaneous coaxial trans-thoracic biopsy should be the first choice in all appropriate cases.

Keywords: Trans-thoracic biopsy, malignant, pneumothorax, hemorrhage, hemoptysis

*This article was published as an oral presentation at the Turkish Thoracic Radiology Association symposium on 20-21 April 2019.

INTRODUCTION

Lung biopsies can be classified into four groups according to the route of access to the lesion: percutaneous transthoracic, bronchoscopic, video-assisted thoracoscopic surgery (VATS), and open surgical biopsies.[1] Bronchoscopic biopsy is limited to centrally located tumors that can be seen through the airways.[2] VATS and open surgical lung biopsies provide larger specimens but have higher morbidity and mortality.[1,3] Ultrasound (US) and computed tomography (CT) are the two most commonly used guidance techniques for percutaneous lung biopsy.[4] Since US waves cannot pass through air-containing lung tissue, US-guided biopsy can only be performed for lesions adjacent to the thoracic wall, and its use is limited.1 CT-guided procedures are the current standard for transthoracic needle biopsy of pulmonary masses.[5,6] It is a less-invasive method with high accuracy and reliability.[7] It often prevents unnecessary surgical procedures with tissue diagnosis. In malignant lesions, it is also preferred to determine the cell type since pathologic diagnosis and cell type determine the treatment modality.[8]

Although PCTTB is a reliable method, complications such as pneumothorax and hemothorax may rarely occur.[9] There are reports of serious complications such as air embolism and rare deaths following a lung biopsy.10

In our study, we aimed to evaluate the diagnostic rates and procedure-related complications of lung masses undergoing CT-guided PCTTB.

METHODS

This retrospective study was conducted at Kırıkkale University Faculty of Medicine according to the principles of the Declaration of Helsinki. Ethics Committee Approval was obtained from Kırıkkale University Clinical Researches Ethics Committee (Date: 03.09.2019, Decision No: 19/07). This article was published as an oral presentation at the Turkish Thoracic Radiology Association symposium on 20-21 April 2019.We retrospectively analyzed 117 patients who underwent CT-guided PCTTB between January 2016 and December 2018. Demographic characteristics, post-procedural diagnosis rates, and complications were evaluated.

For each patient prior to PCTTB, we obtained a low-dose axial CT scan on a 64-detector scanner using multislice computed tomography (MSCT) (Brilliance 64; Philips Medical System, Best, the Netherlands) under the following imaging parameters: 120 kVp, 30 mA per slice, 0.75-second rotation time, and collimation of 8×5 mm. Axial images were scanned with a 2-3 mm section thickness. All PCTTBs were performed by experienced interventional radiologists (AÖ, MHS) using an automated biopsy needle.

The bleeding parameters of all patients were checked before biopsy (INR and platelet count). Patients whose values were not suitable for the procedure (INR>1.5, platelet count< 50,000) were given the necessary treatments, and after the control values were checked, patients with improvement were included in the procedure. Patients taking antiplatelet and anticoagulant drugs such as aspirin and coumadin were discontinued at least 5 days before the procedure. All patients were informed about the purpose, method, and possible complications of the biopsy procedure, and informed consent forms were obtained from all patients.

The PCTTB procedure was started by placing the patient in the appropriate position, in a way to cover the shortest distance, and by placing a metal marker (Figure 1). A local anesthetic was applied to the subcutaneous distance to the entry localization. Repeated control CT sections were obtained to access the lesion. All biopsy procedures were performed with an 18–20-gauge Tru-cut biopsy needle using a 10-15 cm long coaxial needle (Figure 2). The tissue sample was sent to the pathology department in a sterile container containing formol. After the biopsy was completed, control CT sections were obtained to evaluate pneumothorax and/or hemorrhage. The patients were followed up in the clinic, and PA chest radiographs were taken at the second hour. SPSS for Windows 20.0 (SPSS, Inc., Chicago, IL, USA) software program was used for analysis.

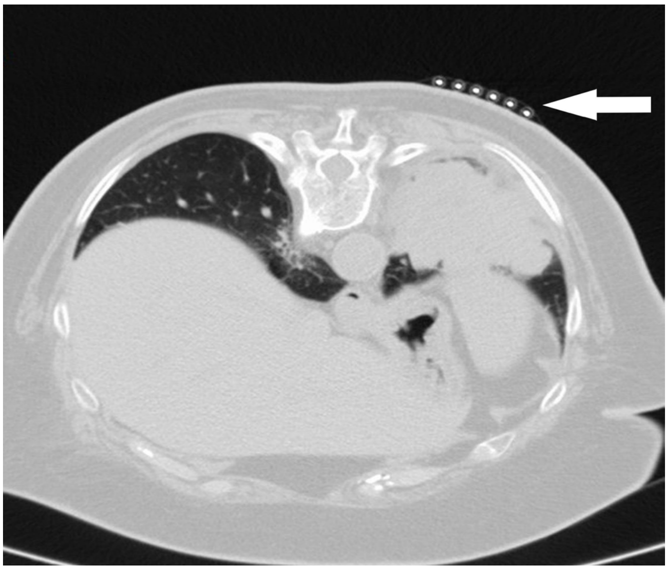

Figure 1. CT-guided PCTTB from left lower lung mass. Preprocedure scan with a grid on the skin is also shown. . (white arrow)

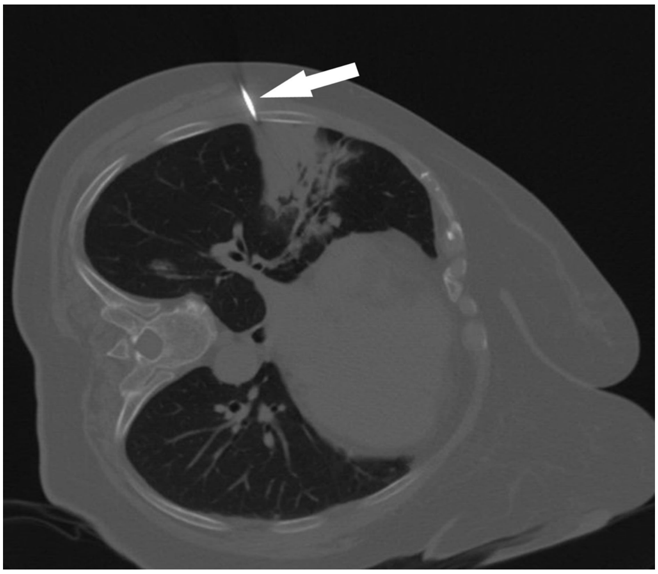

Figure 2. Axial CT scan of mass on the left lung in patient is presented. The outer cannula of a co-axial biopsy device is inserted within the lesion. (white arrow)

RESULTS

Of the 117 patients who underwent PCTTB, 93 were male (mean age 67.9±10.8 years) and 24 were female (mean age 64.2±15.2 years). The pathologic evaluation of three patients was reported as "insufficient material". The diagnostic sensitivity of CT-guided PCTTB was 97.4%. Malignant lesions were detected in 70 patients (59.8%) and benign lesions in 44 patients (37.9%). The most common malignant lesion was adenocarcinoma, while the most common benign lesion was nonspecific findings (Tables 1, 2).

Table 1.

Benign Lesions	Frequency (n)
Non-specific findings (congestion, inflammation, fibrosis...)	30
Anthracosis	4
Pneumonia	3
Necrotizing granulomatous lesion	3
Hamartoma	2
Thymoma	2

Table 2.

Malignant Lesions	Frequency (n)
Adenocarcinoma	32
Squamous cell carcinoma	29
Small cell carcinoma	2
Sarcomatoid	2
Metastasis (colorectal carcinoma, renal cell carcinoma, malignant mesenchymal tumor)	5

The most common complication was pneumothorax, which was observed in 24 (20.5%) patients (Figure 3). A thoracic tube was inserted in three of these patients, while the others were discharged with follow-up. Other complications included hemorrhage in 12 patients (10.3%) and hemoptysis in 14 patients (12%). While mortality in CT-guided biopsy was associated with air embolization in some studies, mortality was not present in our study.

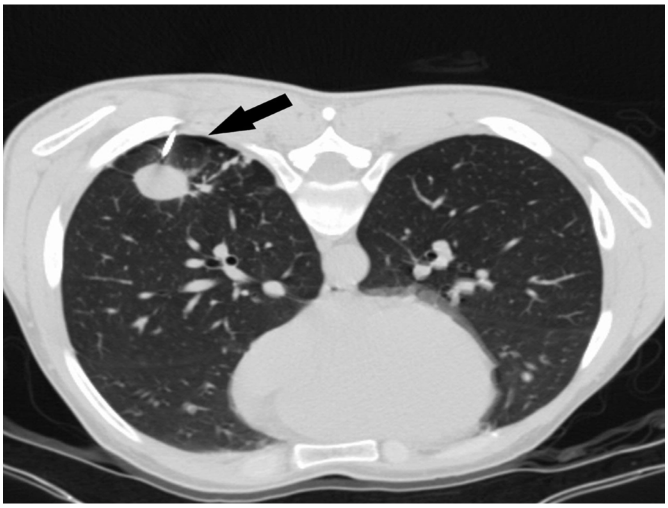

Figure 3. Axial CT scan, Pneumothorax occurring during the procedure is observed. (black arrow)

DISCUSSION

CT-guided PCTTB is currently the most commonly used method for the pathologic diagnosis of pulmonary lesions because of its high diagnostic yield and acceptable complications.[1]

A CT-guided lung biopsy can be performed as a fine needle aspiration or Tru-cut. An aspiration biopsy provides a cytologic diagnosis, while a Tru-cut biopsy provides a tissue diagnosis. The sensitivity in malignant lesions is around 95% in both, whereas in benign lesions, the sensitivity is reported to be 80% with a Tru-cut and 20-50% with an aspiration biopsy. In our study, the pathologic evaluation of three patients was reported as "insufficient material". The diagnostic sensitivity of our study was 97.4%.

The most common complication of transthoracic percutaneous needle biopsy is pneumothorax, with a frequency of 0-61%, and chest tube drainage is required in 1.6% to 17% of pneumothorax cases. Tomiyama[11] published the results of a CT-guided needle biopsy of pulmonary lesions in 9,783 patients. Pneumothorax was the most common complication and occurred in 35% of the 6,881 cases. In the Şahan et al. study, pneumothorax was the most common complication, with 23.8% (20/84).[12] Two of these 20 patients required chest tube drainage. In our study, the rate of pneumothorax was 20.5% (n:24) and the need for a chest tube was 7.3% in these patients, which is consistent with the literature.

Advancing the needle in the parenchyma during breath holding, not crossing the fissure bulla with the needle, and traveling as little as possible in the lung parenchyma are the methods that can be applied to prevent the development of pneumothorax.[13] Recent studies have also reported that post-procedural administration of autologous blood clots through the coaxial needle may also be beneficial.[14]

Pneumothorax develops immediately after the biopsy procedure or within the first hour.[13] Therefore, it is recommended that the patient should be under observation and evaluated for asymptomatic pneumothorax with an outpatient PA chest radiograph.[13] In our study, PA chest radiographs were obtained from the patients who underwent biopsy in the second hour after the procedure.

Pulmonary hemorrhage is the second most common complication, and its frequency has been reported to vary between 5-27% in studies.[3,15] Tuncel et al.[16] found this rate to be 28%. Hemoptysis is another complication and is usually self-limiting.[3] In our study, hemorrhage was observed in 12 patients (10.3%) and hemoptysis in 14 patients (12%).

Other rare complications with high morbidity and mortality include systemic air embolism, pericardial tamponade, and hemothorax, which require a multidisciplinary approach. The mortality rate has been reported to be less than 1% in studies.[1] In our patient group, mortality or the aforementioned major complications were not observed.

Our study has some limitations, and these are retrospective in nature. Other limitations include not specifying the lesion size, localization, and depth distance.

CONCLUSION

CT-guided PCTTB lung biopsies have a high diagnostic rate and acceptable complications. Percutaneous coaxial trans-thoracic biopsy should be the first choice in all appropriate cases.

ETHICAL DECLARATIONS

Ethics Committee Approval

The study was carried out with the permission of Kırıkkale University Faculty of Medicine Clinical Researches Ethics Committee (Date: 03.09.2019, Decision No: 19/07).

Informed Consent

Because the study was designed retrospectively, no written informed consent form was obtained from patients.

Referee Evaluation Process

Externally peer-reviewed.

Conflict of Interest Statement

The authors have no conflicts of interest to declare.

Financial Disclosure

The authors declared that this study has received no financial support.

Author Contributions

All of the authors declare that they have all participated in the design, execution, and analysis of the paper, and that they have approved the final version.

REFERANCES

1. Manhire A, Charig M, Clelland C, et al. Guidelines for radiologically guided lung biopsy. *Thorax.* 2003;58(11):920-936.
2. Herth FJF, Eberhardt R, and Ernst A. The future of bronchoscopy in diagnosing, staging and treatment of lung cancer. *Respiration.* 2006;73(4):399-409.

3. Düzgün F, Tarhan S. Perkütan transtorasik akciğer ve kemik biyopsileri. *Trd Sem.* 2015;(3):182-191.
4. Cheng YC, Tsai SH, Cheng Y, et al. Percutaneous transthoracic lung biopsy: comparison between C-arm cone-beam CT and conventional CT guidance. *Transl Oncol.* 2015;8(4):258-264.
5. Hiraki T, Mimura H, Gobara H, et al. CT fluoroscopy-guided biopsy of 1,000 pulmonary lesions performed with 20-gauge coaxial cutting needles: diagnostic yield and risk factors for diagnostic failure. *Chest.* 2009;136:1612-1617.
6. Brenner DJ, Hall EJ. Computed tomography—an increasing source of radiation exposure. *N Engl J Med.* 2007;357(22):2277-2284.
7. Sivri, M. Bilgisayarlı tomografi eşliğinde transtorasik akciğer biyopsisi yapılan hastaların sonuçlarının değerlendirilmesi ve komplikasyonlara eşlik eden risk faktörlerinin belirlenmesi. 2016
8. Cohen BR, Leitner 0, Ronah R, Guber A, Griffel B, Geiger B: immunocytochemical characterization of lung tumors in fine-needle aspiration. *Cancer.* 1990;66(8):1817-1827.
9. Berquist TH, Bailey PB, Cortese DA, et al. Transthoracic needle biopsy: accuracy and complication in relation to location and type of lesion. *Mayo Clin Proc.* 1980;55(8):475-481.
10. Sinner WN. Complications of percutaneous transthoracic needle aspiration biopsy. *Acta Radiol Diag.* 1976;17(6):813-828.
11. Tomiyama N, Yasuhara Y, Nakajima Y, et al.CT-guided needle biopsy of lung lesions: a survey of severe complication based on 9783 biopsiesin Japan. *Eur J Radiol.* 2006;59(1):60-64.
12. Şahan MH, Inal M, Muluk NB, Doğan A, Atasoy P. The diagnostic value of CT-guided percutaneous Co-axial trans-thoracic biopsy (PCTTB) and evaluation of the pathologic examination. *Current Med. Imaging.* 2019;15(5):479-488.
13. Boskovic T, Stanic J ,Pena-Karan S, et al. Pneumothorax after transthoracic needle biopsy of lung lesions under CT guidance. *J Thorac Dis.* 2014;6(1):99-107.
14. Lang E K, Ghavami R, Schreiner V C, Archibald S, Ramirez J. Autologous blood clot sealto prevent pneumothorax at CT-guided lung biopsy. *Radiology.* 2000;216(1):93-96.
15. Takeshita J, Masago K, Kato R, et al. CT-guided fine-needle aspiration and core needle biopsies of pulmonary lesions: a single center experience with 750 biopsies in Japan. 2015;204(1):29-34.
16. Tuncel P, Ergun O, Çetin N, Türkmenoğlu TT, Durmaz HA, Hekimoğlu B. CT-guided percutaneous transthoracic lung biopsy: one center experience. *Ortadoğu Tıp Dergisi.* 2018;10(1):57-63.

Journal of Radiology in Medicine

Original Article

Doi: 10.51271/JRM-0013

Evaluation of hip angles with magnetic resonance imaging in early stage femoral head osteonecrosis

Mehmet Hamdi Şahan,[1] Duçem Mete[2]

[1]Department of Radiology, Faculty of Medicine, Gaziantep University, Gaziantep, Turkiye
[2]Department of Radiology, Gaziantep Şehitkamil State Hospital, Gaziantep, Turkiye

Received: 01.07.2024 ◆ Accepted:26.07.2024 ◆ Published: 29.07.2024

Cite this article: Şahan MH, Mete D. Evaluation of hip angles with magnetic resonance imaging in early stage femoral head osteonecrosis. *J Radiol Med.* 2024;1(3):46-49.

Corresponding Author: Mehmet Hamdi Şahan, drmehmetsahan@hotmail.com

ABSTRACT

Aims: It was aimed to evaluate the alpha and Wiberg angles of patients with clinical and radiological diagnosis of idiopathic femoral head osteonecrosis (FHO) in comparison with the control group.

Methods: Routine hip MRI (Magnetic resonance imaging)s between January 2022 and May 2024 were examined retrospectively. MRI images diagnosed with early stage (stage I, II according to Ficat and Arlet classification), idiopathic FHO were recorded. A control group matched in age and gender was created. Alpha angle was measured as the angle between the parallel line drawn from the center of the femoral head to the femoral neck in axial MRIs and the line drawn from the transition point between the femoral head and neck in the anterior to the center of the femoral head. Wiberg's central corner angle was measured as the angle between the perpendicular line drawn from the center of the femoral head to the acetabulum and the line connecting the outermost point of the acetabulum in coronal images. Measurements were compared statistically in both groups. $P<0.05$ was considered statistically significant.

Results: A total of 70 hips were examined, including 35 FHO (13 unilateral and 11 bilateral hips) and 35 control groups (3 unilateral and 16 bilateral hips). There was no difference between the groups in terms of age and gender ($P>0.05$). We found statistically significant differences in alpha and Wiberg angles between the FHO and control groups ($P=0.04$, $P=0.025$, respectively). There was no statistically significant difference between stages I and II in terms of alpha and Wiberg angles ($P=0.376$, $P=0.078$, respectively).

Conclusion: These changes in hip angle measurements in this study may explain the cause of idiopathic FHO. We can predict FHO early.

Keywords: Hip, femur head, femur head necrosis, MRI, asetabulum

INTRODUCTION

Osteonecrosis, also known as avascular necrosis of bone, is the death of marrow elements and osteocytes due to deterioration of the vascularity of the bone.[1,2] Femoral head osteonecrosis (FHO) is the most common site and is probably caused by the combination of high loading during standing and poor blood supply.[3,4] There are many potential causes of osteonecrosis, including trauma, steroid use (systemic or local), vasculitis, hyperlipidemia, sickle cell anemia, Gaucher disease, pancreatitis, alcoholism, AIDS, radiation, and embolism. Some cases are classified as idiopathic.[1]

Osteonecrosis can be diagnosed based on characteristic radiographic, Computed tomography, MRI (Magnetic resonance imaging), or radionuclide bone scintigraphy findings.[1] The Ficat and Arlet classification uses a combination of plain radiographs, MRI, and clinical features to stage osteonecrosis of the femoral head.[5,6] It consisted of stages I through.[4,5,6] On MRI, edema in stage I, geographic defect, sclerosis and/or subchondral cysts in stage II are observed. Starting from stage III, morphological changes and degeneration begin to develop in the femoral head.

Alpha angle measurement is the best way to evaluate the abnormal morphology of the anterior femoral head-neck connection in the axial oblique plane. This is a widely used method for evaluation. The alpha angle was first described by Notzli et al.[7] in 2002. Angles greater than 55° are thought to be associated with femoroacetabular impingement.

The central edge angle was defined by Wiberg and provides information about the lateral coverage of the femoral head by the acetabulum in the coronal plane. It measures the femoral head-acetabulum relationship in the coronal plane. While large angle values indicate deep acetabulum, small angle values indicate both protrusion of the femoral head and shallowness of the acetabulum. Here, the angle between the line connecting the center of the femoral head and the lateral edge of the acetabulum and the line drawn perpendicularly from the center of the femoral head is measured.[8]

Hip angle measurements have been frequently examined in femora-acetabular impingement syndromes. To our knowledge, no evaluation has been made on idiopathic FHO. Changes in hip angles (alpha and wieberg angle) are observed in FHO. In this study, we aimed to evaluate the alpha and Wiberg angles of patients with a clinical and radiological diagnosis of stage I-II (which did not cause any change in femoral head morphology) idiopathic femoral head osteonecrosis, in comparison with the control group.

METHODS

This retrospective study was conducted at Gaziantep University. The study was carried out with the permission of the Gaziantep University Clinical Researches Ethics Committee (Date: 12.06.2024, Decision No: 2024/209). All procedures were carried out in accordance with the ethical rules and the principles of the Declaration of Helsinki.

Subjects

Between January 2022 and May 2024, hip MRI examinations were examined. In this study, patients with early stage(stage I, II according to the Ficat and Arlet classification).[5,6] Idiopathic FHO, and clinically and radiologically diagnosed MRI images that did not cause any change in femoral head morphology were included in the study. A control group was created from hip MRI images similar in age and gender, with normal hip MRI examinations.

Exclusion Criteria

Exclusion criteria for the patient and control groups; Patients who were younger than 18 years of age, had distorted hip joint and femoral head configuration on MRI, had stage III and IV osteonecrosis and osteoarthritis in the hip joint, had a history of tumor, trauma, and had surgery were excluded from the study.

Considering similar studies in the literature,[9-11] in order for the volume change between groups to be statistically significant (Cohen's d=0.5), the minimum number of people required in each group should be 35 (α=0.15, 1-β=0.85). In our study, we determined that a total of 70 hip MRI images would be performed, 35 in each group. Power analyses were performed by the Gpower 3.1 program.

MRI Technique and Measurements

All MRI examinations were performed using cranial coil by 3.0 Tesla (T) MRI systems (Ingenia, Philips Healthcare, Best, the Netherlands). The routine hip MRI protocol for the 3.0-T MR machine at Gaziantep University Hospital was as follows:

T1 weighted in the coronal plane (TR ms/TE ms; 500/20, FOV 250x396 mm and matrix 300×421 mm) were obtained using a 4-mm slice thickness and 0,5-mm intersection gap; and 35-40 coronal sections were obtained. T2-SPAIR (Spectral Attenuated Inversion Recovery) weighted in the axial plane (TR ms/TE ms; 700/62, FOV 275x350 mm and matrix 31×310 mm) were obtained using a 4-mm slice thickness and 0,5-mm intersection gap; and 35-40 axial sections were obtained.

The alpha angle was measured on the axial T2-(SPAIR) weighted MRI images by calculating the angle between the parallel line drawn from the center of the femoral head to the femoral neck and the line drawn from the transition point between the femoral head and femoral neck in the anterior to the center of the femoral head (Figure 1).[8,10,12] Central corner angle of Wiberg was measured on the coronal T1-weighted images by calculating the angle between the perpendicular line drawn from the center of the femoral head to the acetabulum and the line connecting the outermost point of the acetabulum (Figure 2).[8,10,12] All measurements were made by one radiologist (D.M.), and MRIs were determined by consensus by two radiologists (Duçem M, Şahan MH).

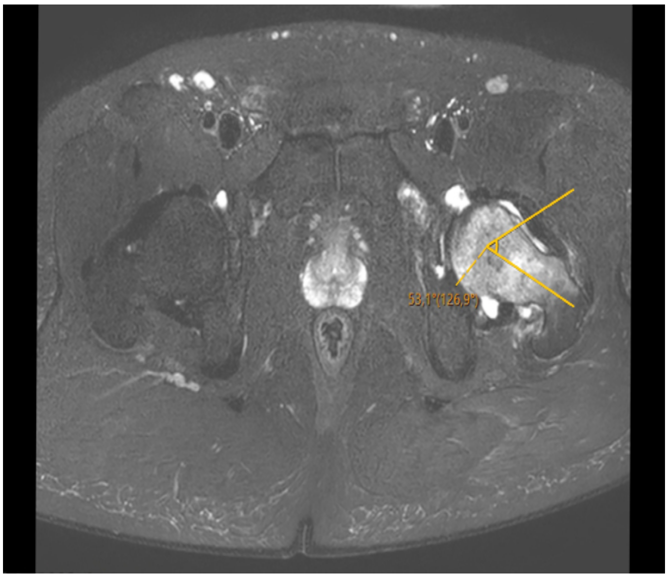

Figure 1. 44-year-old man, stage I osteonecrosis of the left hip, alpha angle measurement on the axial T2 SPAIR weighted image

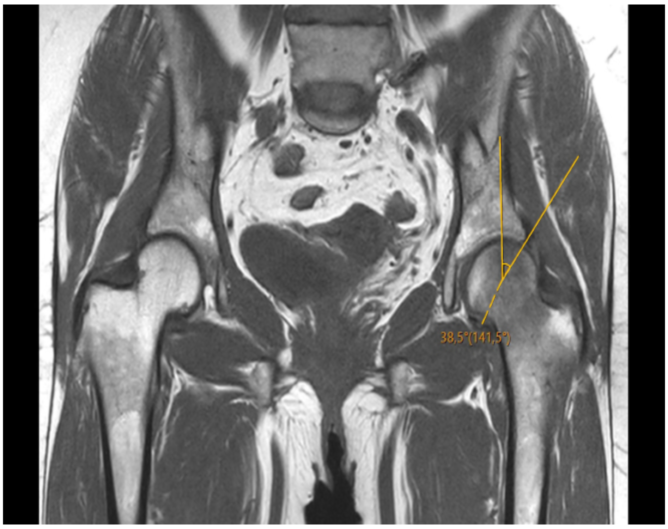

Figure 2. 48-year-old woman, stage I osteonecrosis of the left hip, Wieberg angle measurement on the coronal T1 weighted image

Statistical Analysis

Version 20.0 of the Statistical Package for the Social Sciences (SPSS, INC, an IBM Company, Chicago, Illinois, United States) software was used for the analysis. Descriptive statistics are presented as mean, standard deviation, minimum and maximum. A chi-square test, independent samples t-test, Mann whitney U test. A p-value < 0.05 was considered as statistical significance.

RESULTS

A total of 70 hips were examined, including 35 FHO (13 unilateral and 11 bilateral hips) and 35 control groups (3 unilateral and 16 bilateral hips). There was no difference between the groups in terms of age and gender (p >0.05), (Table). There was no significant difference between hip directions (right-left). (FHO; 17 right, 18 left and control group; 18 right and 17 left hips). Of the FHO patients, 7 were stage I and 28 were stage II. We found statistically significant differences in alpha and Wiberg angles between the FHO and control groups (p=0.04, p=0.025, respectively), (Table). There was no statistically significant difference between stages I and II in terms of alpha and Wiberg angles (p=0.376, p=0.078, respectively).

Table. Comparison of age, gender, alpha angles and Wiberg angles of femoral head osteonecrosis and control group

	FHO	Control group	p value
Age (years)	46.89±12.3	47.2±13.89	0.939*
Gender: M/F	26/9	23/12	0.434*
Alpha angle mean (min-max)	50.22±6.3	54.1±8.9	0.04**
	(37.9-63.7)	(38-70)	
Wiberg angle mean (min-max)	40.89±7.8	36.87±6.7	0.025**
	(25-58)	(28.1-54.5)	

FHO: Femoral head osteonecrosis, M: Male, F: Female
* P value shows the results of Man Whitney U test
**P value shows the results of Chi-square test
***P value shows the results of independent samples t-test

DISCUSSION

FHO is an increasingly common cause of hip disability and poses a significant diagnostic and treatment challenge.[4] The cause of FHO can be clearly identified in patients with direct damage to the bony vascular system, bone or marrow.[9,13] However, the pathogenesis of FHO remains a matter of debate in many patients as sufficient information is still lacking. In addition to the known identifiable causes of FHO, some cases (30%) are defined as idiopathic because the pathology cannot be precisely determined.[9,13,14]

In our study, we found that the alpha angle was low and the Wieberg angle was significantly high on MRI in stage I and II FHO. Studies in the literature on alpha and Wiberg angle are related to femoroacetabular impingement.[8,10,12] Alpha angle is the angle between the parallel line drawn from the center of the femoral head to the femoral neck and the line drawn from the transition point between the femoral head and neck in the anterior to the center of the femoral head. Above 55° is considered as a cam type femoral acetabular impingement lesion.[10,15,16] Wiberg angle is defined by measuring the angle between the line connecting the lateral edge of the acetabulum to the center of the femoral head and the line drawn perpendicular to the center of the femoral head.[8,10,12] While larger angles indicate a deep acetabulum, smaller angle values indicate both protrusion of the femoral head and shallowness of the acetabulum. The normal range is 25-39°, over 40° indicates excessive coverage, between 25°-17° indicates borderline dysplasia, and below 17° indicates severe dysplasia.[8,10,12]

Hip angles have not been studied with FHO before. It can be assumed that FHO, one third of which have no clear underlying etiology, has a direct correlation with changes in the alpha and Wieberg angles of the Hip. More comprehensive studies can be conducted that include different angle measurements.

Limitations

This study had some limitations. First, the study had a single-center, retrospective design with a relatively small sample size. Second, measurements included routine hip MRI protocols. Finally, the variability of the intraobserver and the interobserver measurements were not evaluated.

CONCLUSION

These changes in angle measurements in this study may explain the cause of idiopathic FHO. In the study results, we found that the alpha angle was low (abnormal morphology of the femoral head-neck connection) and the Wieberg angle was high (associated with the deep acetabulum). Based on these results measured on MRI, we can predict femoral head osteonecrosis early. More multicenter studies with larger series of FHO patients are needed to fully elucidate these findings and their clinical significance.

ETHICAL DECLARATIONS

Ethics Committee Approval

The study was carried out with the permission of the Gaziantep University Clinical Researches Ethics Committee (Date: 12.06.2024, Decision No: 2024/209).

Informed Consent

Because the study was designed retrospectively, no written informed consent form was obtained from patients.

Referee Evaluation Process

Externally peer-reviewed.

Conflict of Interest Statement

The authors have no conflicts of interest to declare.

Financial Disclosure

The authors declared that this study has received no financial support.

Author Contributions

All of the authors declare that they have all participated in the design, execution, and analysis of the paper, and that they have approved the final version.

REFERENCES

1. Crim J, Layfield LJ, Stensby JD, Schmidt RL. Comparison of radiographic and pathologic diagnosis of osteonecrosis of the femoral head. *AJR Am J Roentgenol*. 2021;216(4):1014-1021.
2. Klein M, Bonar S, Freemont T, Vinh T, Lopez-Ben R, Siegel H. Traumatic and circulatory alterations of bone. Atlas of non-tumour pathology, non-neoplastic diseases of bones and joints: American Registry of Pathology And Armed Forces Institute Of Pathology. Washington DC. 2011;1:299-354.
3. Glickstein MF, Burk D, Schiebler M, et al. Avascular necrosis versus other diseases of the hip: sensitivity of MR imaging. Radiology. 1988;169(1):213-215.
4. Stoica Z, Dumitrescu D, Popescu M, Gheonea I, Gabor M, Bogdan N. Imaging of avascular necrosis of femoral head: familiar methods and newer trends. *Curr Health Sci J*. 2009;35(1):23.
5. Jawad MU, Haleem AA, Scully SP. In brief: ficat classification: avascular necrosis of the femoral head. Clin Orthop Relat Res. 2012;470(9):2636-2639.
6. Ficat RP. Necrosis of the femoral head. Ischemia and necross of bone bone. Williams and Wilkins. 1980;17:171-182.
7. Nötzli H, Wyss T, Stoecklin C, Schmid M, Treiber K, Hodler J. The contour of the femoral head-neck junction as a predictor for the risk of anterior impingement. *J Bone Joint Surg Br*. 2002;84(4):556-560.
8. Matcuk Jr GR, Price SE, Patel DB, White EA, Cen S. Acetabular labral tear description and measures of pincer and cam-type femoroacetabular impingement and interobserver variability on 3 T MR arthrograms. *Clin Imaging*. 2018;50:194-200.
9. Günay C, Özçelik A. Is Stage 2 idiopathic osteonecrosis of the hip joint associated with version angles on imaging methods? *Jt Dis Relat Surg*. 2021;32(3):611.
10. Kültür T, İnal M. Evaluation of hip angles with magnetic resonance imaging in femoroacetabular impingement syndrome. *N Engl J Med*. 2020;3(3):225-230.
11. Mitchell D, Rao VM, Dalinka MK, Spritzer C, Alavi A, Steinberg M, et al. Femoral head avascular necrosis: correlation of MR imaging, radiographic staging, radionuclide imaging, and clinical findings. *Radiology*. 1987;162(3):709-715.
12. Keogh MJ, Batt ME. A review of femoroacetabular impingement in athletes. *Sports Med*. 2008;38:863-878.
13. Aldridge JM, Urbaniak JR. Avascular necrosis of the femoral head: etiology, pathophysiology, classification, and current treatment guidelines. *Am J Orthop*. 2004;33(7):327-332.
14. Zeng J, Zeng Y, Wu Y, Liu Y, Xie H, Shen B. Acetabular anatomical parameters in patients with idiopathic osteonecrosis of the femoral head. *J Arthroplasty*. 2020;35(2):331-334.
15. Allen D, Beaulé P, Ramadan O, Doucette S. Prevalence of associated deformities and hip pain in patients with cam-type femoroacetabular impingement. *J Bone Joint Surg Br*. 2009;91(5):589-594.
16. Hatakeyama A, Utsunomiya H, Nishikino S, et al. Predictors of poor clinical outcome after arthroscopic labral preservation, capsular plication, and cam osteoplasty in the setting of borderline hip dysplasia. *Am J Sports Med*. 2018;46(1):135-143.

Journal of Radiology in Medicine

Original Article

Doi: 10.51271/JRM-0014

Evaluation of stress levels in adult patients waiting for ultrasonography examination in radiology unit

Pelin Zeynep Bekin Sarıkaya,[1] Atike Tekeli Kunt,[2] Gözde Çolakoğlu,[3] Yaren Altunkaynak,[3] Ahmet Cemil Ülger,[3] Muhammed Eymen Özerdem,[3] İrem Acar[3]

[1]Department of Radiology, Faculty of Medicine, Kırıkkale University, Kırıkkale, Turkiye
[2]Department of Cardiovascular Surgery, Faculty of Medicine, Kırıkkale University, Kırıkkale, Turkiye
[3]Undergraduate Student, Faculty of Medicine, Kırıkkale University, Kırıkkale, Turkiye

Received: 28.06.2024 ◆ **Accepted**: 26.07.2024 ◆ **Published**: 29.07.2024

Cite this article: Bekin Sarıkaya PZ, Tekeli Kunt A, Çolakoğlu G, et al. Evaluation of stress levels in adult patients waiting for ultrasonography examination in radiology unit. *J Radiol Med.* 2024;1(3):50-53.

Corresponding Author: Pelin Zeynep Bekin Sarıkaya, zeybekin@hotmail.com

ABSTRACT

Aims: In this study, we aimed to reveal the level of anxiety and depression of patients waiting in line for ultrasonography in the Radiology unit with the hospital anxiety and depression scale (HAD) and to reveal its relationship with patient characteristics and waiting characteristics.

Methods: The study was conducted with 105 patients waiting for ultrasonography in Kırıkkale University Faculty of Medicine, Department of Radiology between January 2024 and March 2024. Data were collected from the patients before the procedure using a patient identification form and the hospital anxiety and depression scale.

Results: No significant correlation was found between the gender and age of the patients, the internal and surgical departments, the time waiting in the hall, the number of days waiting for the appointment and the results of the hospital anxiety and depression scale ($p>0.05$). We found a significant correlation between the educational level of the patients and the hospital anxiety depression scale score ($p<0.05$).People with basic education had higher HAD scale scores than other educational groups. In this study, we found a relationship between patient education levels and hospital anxiety depression scale.

Conclusion: Hospitals are places that can cause stress, anxiety and depression in patients. The management of these emotions is, of course, closely related to our personal characteristics and educational status. It should be kept in mind that unnecessary anxiety and long-lasting concerns of patients can be eliminated with analytical approaches and understanding the etiology.

Keywords: Ultrasonography; stress; anxiety; depression; HAD.

* This study was presented at the 2nd international Medical Student Symposium of Kırıkkale University Faculty of Medicine on 28.05.2024 in Kırıkkale.

INTRODUCTION

Stress describes a series of reactions that arise from the human emotional state, which can be triggered by external factors, to maintain homeostatic balance. Anxiety occurs when individuals are exposed to stress for a prolonged period of time.[1] Anxiety and depression are two emotional states that sometimes share basic components. Anxiety is a multi-systemic response that is perceived as a threat by individuals.[2] Unlike stress, anxiety is not a momentary but an ongoing experience. If this continuous state of stress is not eliminated, it may result in depression. Depression involves a negative mood accompanied by negative perceptions of self, often resulting in withdrawal from interpersonal relationships and life, and may result in uncontrolled behaviors aimed at harming self and others.[3] Anxiety and depression are co-morbid conditions in terms of health risks. Anxiety and depression are co-morbid conditions in terms of health risks. If their diagnosis and treatment are inadequate, they may predispose to comorbid conditions that may be fatal in the long term.[4] Therefore, it is important for public health that the causes of anxiety and depression are identified and eliminated if possible. We think that hospitals trigger anxiety and depression as one of the conditions that lead to this condition. In this study, we aimed to reveal the level of anxiety and depression in patients waiting in line for ultrasonography in the Radiology unit by using a previously defined scale (Hospital Anxiety and Depression Scale, HAD) and to reveal its relationship with patient characteristics and waiting characteristics.[5]

METHODS

The study was carried out with the permission of Kırıkkale University Non-interventional Researches Ethics Committe (Date: 14.02.2024, Decision No:2024.02.12). All procedures were carried out in accordance with the ethical rules and the principles of the Declaration of Helsinki. Informed consent was obtained from all patients participating in the survey study.

Patient Selection

Patients who were waiting for ultrasonography at Kırıkkale University Faculty of Medicine, Department of Radiology between January and March 2024 were selected to participate in our study. Exclusion criteria were determined. These were determined as patients under 18 years of age, patients with stretchers, patients with confusion, inpatients, and patients referred from the emergency department. Patients who did not meet the exclusion criteria were informed in the waiting room and those who wanted to participate were randomly selected and included in the study.

Data Collection

Among the patients waiting in the ultrasonography waiting room at Kırıkkale University Faculty of Medicine, Department of Radiology, those who did not meet the exclusion criteria were randomly informed and a patient information form was filled out for those who agreed to participate in the study. Afterwards, demographic data of the patients were noted. First, a patient identification form was filled out and then the HAD was administered. In the patient information form; the patient's age, gender, education level (no education, basic education, university and higher education level), occupation (student, working, not working), the department to which the patient was referred to Radiology for USG (Internal departments, Surgical departments), time taken to reach the appointment (unit: day), waiting time in the hall (unit: minute) were filled in. Data collection was terminated after reaching the desired number of patients. The scoring of the HAD questionnaire results was summed and a grouping of 1-4 was created and recorded in the table with other information.

Statistical Analysis

SPSS for 21.0 (SPSS; IBM Inc, Chicago, IL) was used for statistical analysis. Mann whitney U test was used to compare between two groups. Chi-square test was used to compare nominally classified data in groups. $p<0.05$ was considered statistically significant.

RESULTS

A total of 105 patients were included in our study. There were 61 female (58%) and 44 male (42%) patients. Patient ages ranged between 21-76 years. We found no significant correlation between the gender and age of the patients and the results of the hospital anxiety depression scale ($p>0.05$).

We did not find a significant relationship between the occupation of the patients and the results of the hospital anxiety depression scale ($p>0.05$). We did not find a significant relationship between the internal and surgical departments the patients came from and the results of the hospital anxiety and depression scale ($p>0.05$).

We did not find a significant correlation between the time the patients waited in the hall and the hospital anxiety depression scale result ($p>0.05$).We did not find a significant correlation between the number of days patients waited for an appointment and the results of the hospital anxiety and depression scale ($p>0.05$).

We found a significant correlation between the educational level of the patients and the hospital anxiety depression scale score ($p<0.05$).People with basic education had higher HAD scale scores than other educational groups (Figure).

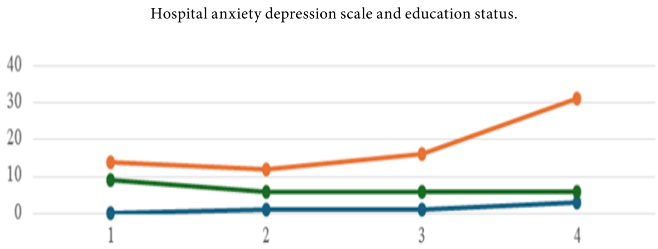

Figure. The relationship between the CFS scale and education level
*Red: Basic Education, Blue: None, Green: Higher Education

DISCUSSION

Stress is one of the most fought public health problems today. In addition, anxiety and depression accompanying the stress of patients affect both mental and physical conditions, causing psychophysiological stress reactions and various reactions. This impairs mental health as well as physical health and affects many conditions, especially the recovery period. It also causes violence in hospitals.[6] It is important to understand the cause of these undesirable situations that cause stress in healthcare workers in order to prevent them. Various studies have shown that hospitals increase the stress levels of patients.[7] In this study, in which we aimed to reveal the level of anxiety and depression of patients waiting in the radiology unit with the previously defined scale (Hospital Anxiety and Depression Scale) and to reveal its relationship with the department requested, gender, age, educational status, appointment time and waiting time; we obtained significant results between the education levels of the patients and their anxiety levels. As a result of our study, it was found that patients with basic education had much higher anxiety levels than patients without basic education and patients with higher education. In the study conducted by Samudio-Cruz et al.,[8] they discussed that the level of education regulates the presence of depression and anxiety in post-stroke patients. The hospital anxiety and depression scale, which we also used in our study, is one of the scales used and a negative relationship was found between education and anxiety score and depression score. As a result, they obtained data suggesting that higher education level decreased the risk of depression and anxiety. In a study conducted by Arslantaş et al., the level of hopelessness and social support and the factors affecting them were investigated in inpatients, and as a result, it was found that low educational level increased the hopelessness score. Kılınç et al.[9] conducted a study on anxiety and depression in patients with Familial Mediterranean Fever (FMF). As a result of the study, it was found that patients with FMF had mild depression and moderate anxiety scores and higher education level was associated with lower anxiety level.[10] In the study by Liang et al.[11] on the evaluation of preoperative psychological status of patients undergoing liver transplantation, no correlation was found between educational level and preoperative anxiety and depression levels in contrast to our study. Increasing the level of education is of course very important in coping with negative emotions and these results tell us that there is a relationship between the level of education and mental and physical health in societies.

In our study, we did not obtain significant results between the departments requested and anxiety levels. This made us think that other sociodemographic reasons such as anxiety, stress due to not knowing what to expect, and the importance of coming for diagnosis or control may affect our mood in the foreground rather than which department the patients come from. Kayahan and Sertbaş examined the relationship between anxiety-depression levels and stress coping styles in patients hospitalized in internal and surgical clinics. As a result, unlike our study, the mean score of patients hospitalized in surgical clinics was found to be significantly higher than that of patients hospitalized in internal clinics.[7] This finding is compatible with the findings of Kırkpınar et al.[12]

In our study, we could not define any correlation between the gender of the patients and their anxiety levels. In the study conducted by Karadeniz et al. no correlation was found between gender and anxiety levels.[13] In the study conducted by Arslantaş et al.[14] scales such as Becker hopelessness scale (BHS) and multidimensional perceived social support scale (MSPSS) were used, and in both of these scales, the relationship between gender and anxiety levels of patients could not be shown. In the study conducted by Çelik et al.[9] we found that anxiety levels in women were higher than in men according to BHS, but there was no significant difference. We did not find a significant result between the occupations and anxiety levels of the patients. In the study conducted by Karadeniz et al.[13] we found that there was no significant relationship between the occupations and anxiety levels of the patients. This may be due to the lack of diversification of occupational groups. Studies with wider participation are needed.

In the study by Khairy Gad et al. on the prevalence and related determinants of depression, anxiety and stress in COVID-19 patients in South Sinai, Egypt, no significant relationship was found between anxiety and age, similar to ours.[15] Again, in the study titled factors affecting anxiety, depression and stress in patients with hepatocellular carcinoma during the COVID-19 Outbreak by Akbulut et al.[16] Depression anxiety stress scale (DASS-21) and Coronavirus anxiety scale (CAS) were applied to the patients. In their results, in contrast to our study, determinants including the age factor were found to be significant for the DASS total. The data obtained in the Anxiety in Patients with Neovascular Age-Related Macular Degeneration study by Orly Weinstein et al.[17] The rates of patients with anxiety were compared between groups using univariate analysis and multivariate logistic regression model. As a result, they found that the age factor had a significant relationship with anxiety level in contrast to our study.In the study conducted by Oflaz et al.[18] it was aimed to determine the frequency of anxiety and depression symptoms in inpatients and contrary to our study, waiting time was found to be more anxiety and depressive especially in inpatients. In our study, we did not find a significant correlation between waiting time and anxiety and depression scale results. This may be related to the short waiting time for appointments for ultrasonography in our hospital. Wu et al. examined the effect of different preoperative waiting times on anxiety and pain levels in patients undergoing outpatient surgery for breast diseases and found that preoperative anxiety and pain levels of patients undergoing outpatient breast surgery increased with the prolongation of preoperative waiting time.[19] Pontone et al.[20] examined the tolerance and anxiety levels of patients waiting for endoscopy depending on the waiting time and showed that there was no significant relationship as a result of this study. Silva et al.[21] evaluated the relationship between anxiety symptoms and stress in patients waiting for kidney transplantation and found that stress and anxiety were common in patients on the waiting list. Lamba et al.[22] examined the relationship between waiting time for radiation therapy appointment and patient-reported pain and anxiety and found that daily waiting time may play a role in the pain and/or anxiety experienced by cancer patients during radiotherapy.

Limitations

Of the study are including the small number of patients, and the fact that we did not elaborate in detail on the clinical section in which they referred. In addition, the fact that they did not undergo psychiatric examination can also be counted among the limitations. Different contributions to the literature can be made with a larger number of patients.

CONCLUSION

In this study, we found a relationship between patients' education levels and the hospital anxiety and depression scale. Hospitals are places that can cause stress, anxiety and depression in patients. The management of these emotions is, of course, closely related to our personal characteristics and educational status. It should be kept in mind that unnecessary anxiety and long-lasting concerns of patients can be eliminated with analytical approaches and understanding the etiology.

ETHICAL DECLARATIONS

Ethics Committee Approval

The study was carried out with the permission of Kırıkkale University Non-interventional Researches Ethics Committe (Date: 14.02.2024, Decision No:2024.02.12).

Informed Consent

All patients signed and free and informed consent form.

Referee Evaluation Process

Externally peer-reviewed.

Conflict of Interest Statement

The authors have no conflicts of interest to declare.

Financial Disclosure

The authors declared that this study has received no financial support.

Author Contributions

All of the authors declare that they have all participated in the design, execution, and analysis of the paper, and that they have approved the final version.

REFERENCES

1. Fellahoğlu Z. Akıl Sağlığı ve Psikiyatri Hemşireliği. *Inşirah Sahaf.* 1996;1:15-20.
2. Clark LA, Watson D. Tripartite model of anxiety and depression: psychometric evidence and taxonomic implications. *J Abnorm Psychol.* 1991;100(3):316.
3. Fiske A, Wetherell JL, Gatz M. Depression in older adults. *Annu Rev Clin Psychol*. 2009;5:363-389.
4. Carpiniello B, Lai G, Pariante CM, Carta MG, Rudas N. Symptoms, standards of living and subjective quality of life: a comparative study of schizophrenic and depressed out-patients. *Acta Psychiatr Scand*. 1997;96(4):235-241.
5. Aydemir Ö, Güvenir T, Kuzey L, Kültür S. Hastane anksiyete ve depresyon ölçeği Türkçe formunun geçerlilik ve güvenilirlik çalışması, *Turk Psikiyatri Derg.* 1997;8(4):280-287.
6. Kılıç C, Figen İ. Acil tıp çalışanlarında travmatik stres: yaş ve eğitimin koruyucu etkisi. *Turk Psikiyatri Derg*. 2015;26(4):236-241.
7. Kayahan M, Sertbaş G. Dahili ve cerrahi kliniklerde yatan hastalarda anksiyete-depresyon düzeyleri ve stresle başa çıkma tarzlar arasındaki ilişki. *Anadolu Psikiyatri Derg.* 2007(8):113-120.
8. Samudio-Cruz MA, Toussaint-González P, Estrada-Cortés B, et al. Education level modulates the presence of poststroke depression and anxiety, but it depends on age. *J Nerv Ment Dis*. 2023;211(8):585-591.
9. Arslantaş H,Adana F, Kaya F, Turan D. Yatan hastalarda umutsuzluk ve sosyal destek düzeyi ve bunları etkileyen faktörler. *Florence Nightingale J Nurs*. 2010;18(2):87-97.
10. Kilinc OC, Kilinc A, Azman FN, et al. Anxiety and depression among patients with familial Mediterranean fever. *Z Rheumatol*. 2024;83:236-241.
11. Liang P, Gao X, Yin J. Assessment of preoperative psychological state of patients with liver transplantation. *Zhonghua Yi Xue Za Zhi*. 2008;88(43):3045-3048.
12. Kırpınar İ, Coşkun İ, Aydın N, Özer H. Bir üniversite hastanesinde konsültasyonla tanınan depresyonların özellikleri. 30. National Psychiatry Congress Book. 1994;2:143-146.
13. Karadeniz G, Tarhan S, Yanıkkerem E, Dedeli Ö, Kahraman E. Manyetik rezonans ve bilgisayarlı tomografi öncesi hastalarda anksiyete ve depresyon. *Klinik Psikiyatri*. 2008;11(2):77-83.
14. Çelik, HC, Acar T. Kronik hemodiyaliz hastalarında depresyon ve anksiyete düzeylerinin çeşitli değişkenlere göre incelenmesi. *Fırat Tıp Derg.* 2007;12(1): 23-27.
15. Gad BK, Arafa MA, Attia AM, Farahat A, Abdou M. Depression, anxiety, and stress among COVID-19 patients in South Sinai, Egypt: prevalence and associated predictors. *Sci Rep*. 2023;13(1):19193.
16. Akbulut S, Tamer M, Kucukakcali Z, et al. Factors affecting anxiety, depression, and stress among patients with hepatocellular carcinoma during COVID-19 pandemic. *Eur Rev Med Pharmacol Sci.* 2023;27(2):704-712.
17. Weinstein, O, Cohen AD, Levy J, et al. Anxiety in patients with neovascular age-related macular degeneration. *Ophthalmic Epidemiol.* 2023;30(3):286-292.
18. Oflaz F, Vural H. Yatan hastaların anksiyete ve depresyon düzeyleri ve ilişkili faktörlerin incelenmesi. *SDÜ Tıp Fak Derg.* 2010;17(1):1-7
19. Wu B, Wang HJ, Yang XP, Zhong ZH. The influence of preoperative waiting time on anxiety and pain levels in outpatient surgery for breast diseases. *J Patient Saf.* 2024;20(2):105-109.
20. Pontone S, Tonda M, Brighi M, Florio M, Pironi D, Pontone P. Does anxiety or waiting time influence patients' tolerance of upper endoscopy? *Saudi J Gastroenterol*. 2015;21(2):111-115.
21. Silva AN, Moratelli L, Costa AB, et al. Waiting for a kidney transplant: association with anxiety and stress. *Transplant Proc*. 2014;46(6):1695-1697.
22. Lamba N, Niemierko A, Martinez R, Leland P, Shih HA. The Interaction of waiting time and patient experience during radiation therapy: a survey of patients from a tertiary cancer center. *J Med Imaging Radiat Sci*. 2020;51(1):40-46.

Journal of Radiology in Medicine

Case Report

Doi: 10.51271/JRM-0015

Brain abscess mimicking an intracranial mass on radiologic examinations: a case report

Özge Sevimoğlu[1], Ahmet Melih Erdoğan[1], Alemiddin Özdemir[1], Pelin Zeynep Bekin[2] Sarıkaya, Ayşegül Tuna[3], Mahi Balcı,[4] Mustafa Öğden,[1] Bülent Bakar[1]

[1]Department of Neurosurgery, Faculty of Medicine, Kırıkkale University, Kırıkkale, Turkiye
[2]Department of Radiology, Faculty of Medicine, Kırıkkale University, Kırıkkale, Turkiye
[3]Department of Infectious Diseases, Faculty of Medicine, Kırıkkale University, Kırıkkale, Turkiye
[4]Department of Pathology, Faculty of Medicine, Kırıkkale University, Kırıkkale, Turkiye

Received: 20.04.2024 ◆ **Accepted**: 03.06.2024 ◆ **Published**: 29.07.2024

Cite this article: Sevimoğlu Ö, Erdoğan AM, Özdemir A, et al. Brain abscess mimicking an intracranial mass on radiologic examinations: a case report. *J Radiol Med*. 2024;1(3):54-57.

Corresponding Author: Ahmet Melih Erdoğan, ahmetmelih.erdogan76@gmail.com

ABSTRACT

A 49-year-old woman who had a headache for ten days was evaluated in the emergency department. Because the physical examination was normal, an intracranial mass was suspected, and brain computed tomography (CT) revealed an edematous intracranial lesion with an 8.3-millimeter shift in the right occipito-parietal region. In venous blood samples, leukocyte count was 17360 µL (normal range: 4000-10000 µL), C-reactive protein level was 9.42 mg/L (normal range:0-5 mg/L), procalcitonin 0.027 ng/ml (normal range:0-0.05 ng/ml). Choline/NAA (N-acetyl aspartate) peaks that may be in favor of malignancy were obtained in the mentioned lesion in brain MR-spectroscopy images. Contrast-enhanced CT scan of the thorax, abdomen, and pelvis revealed no tumor focus. She underwent a right occipital craniotomy. After opening the mass capsule, a yellow-green, thick, odorless purulent material discharged. Gram-positive diplococci were detected in the emergency smear preparations of this purulent material and "*Streptococcus porcinus*" growth was detected in the subsequent culture. After the normalization of blood biochemistry values and marked improvement in brain MR images, the infectious diseases department terminated antibiotic treatment at the end of the fifth month. As seen in this patient, radiologic imaging may sometimes not be sufficient to make the correct diagnosis and may lead to different diagnoses.

Keywords: Headache, brain abscess, MR-spectroscopy

INTRODUCTION

Brain tumors are mainly divided into primary tumors and metastases. Metastases constitute 20-40% of central nervous system (CNS) tumors in different series. Other lesions that occupy intracranial space and can be confused with tumors on radiological imaging are brain abscesses.[1] Clinical evaluation, laboratory analyses, and radiological imaging methods are used in the differentiation and diagnosis of brain tumors and other intracranial space-occupying lesions.[2] Radiologic imaging is very helpful for diagnosis, but they are insufficient to diagnose definitively when evaluated alone.[3] Among laboratory analyses, tumor markers can be used to support the diagnosis of brain tumors. Still, most of them are elevated in benign and malignant diseases and do not allow the differentiation of these conditions.[4] Therefore, it is still difficult to distinguish between these three entities today.In this case report, we discuss a patient who was thought to have a glial brain tumor after all laboratory analyses and radiological imaging but was found to have a brain abscess during surgery.

CASE

A 49-year-old woman who had a headache for ten days and whose pain had intensified for the last day was evaluated in the emergency department. Neurologic examination revealed that vital values were normal, consciousness was clear, coherent, and oriented, Glasgow Coma Scale (GCS) score was 15/15, pupils were isochoric, and reactive, cranial nerve examination was normal, nuchal rigidity was absent, but she had hemiparesis on the left side of the body (left upper and lower extremity muscle strengths total 4/5). Physical examination of the patient revealed that lung sounds were natural, with no rales or rhonchi; the abdominal examination was comfortable, with no signs of tenderness, defense, or rebound. In addition, oropharyngeal redness or postnasal discharge suggestive of upper respiratory tract infection was not detected. In addition, it was learned that there was no foul-smelling urine or dysuria suggestive of urinary tract infection, but he had left upper 1st molar caries for a long time but had not received any treatment for it.

Intracranial mass was suspected with the present findings and brain computed tomography (CT) performed in the emergency department revealed an edematous intracranial lesion with an 8.3-millimeter shift in the right occipito-parietal region (Figure 1A). In venous blood samples, hemoglobin (HGB) level was 11.7 g/dl (normal range 11-15 g/dL), leukocyte (WBC) count was 17360/µl (normal range 4000-10000 µl), C-reactive protein (CRP) level was 9.42 mg/L (normal range 0-5 mg/L), procalcitonin 0.027 ng/ml (normal range 0-0.05 ng/ml), serum sodium (Na) 125 mmol/L (normal range 136-145 mmol/ml). The patient received 16 mg dexamethasone, 1000 mg levetiracetam, and 40 mg pantoprozole intravenously in the emergency department.

Diffusion MRI images show an area of diffusion restriction in the right occipital region (Figure 1B, Figure 1C). Contrast-enhanced MR revealed a large cystic tumor in the right occipital lobe, with diffuse edema around it, measuring approximately 4 cm in diameter at its widest point, with a heterogeneous internal structure and peripheral weighted contrast enhancement (Figure 1D, Figure 1E, Figure 1F). In addition, ventricular compression secondary to edema and leftward shift of midline structures were observed.

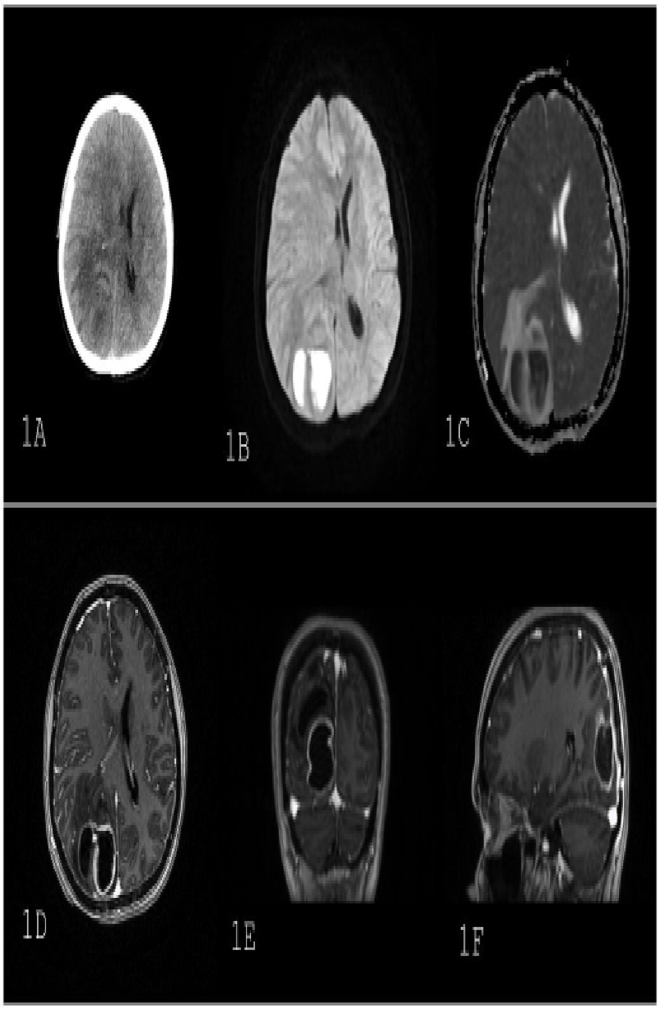

Figure 1. Preoperative brain CT shows a mass lesion located in the right occipital lobe, hypodense in the middle, surrounded by edema, and causing effacement of the right lateral ventricle. (1A). Diffusion MRI images show an area of diffusion restriction in the right occipital region (1B, 1C). Contrast-enhanced brain MRI images show widespread edema in the posterior section of the right cerebral hemisphere and an appearance consistent with a cystic mass lesion with contrast enhancement of the walls at this area level (1D, 1E, 1F)

In brain MR-spectroscopy images performed, significant choline-creatinine, and choline/NAA (N-acetyl aspartate deficiency) peaks that may be in favor of malignancy were obtained in the mentioned lesion area in the left occipital lobe. In addition, TTP (peak time), CBV (cerebral blood volume), CBF (cerebral blood flow), and MTT (mean transit time) values were obtained in the right occipital lobe on brain MR-perfusion images, and a patchy diffusion restriction area was detected in the right occipital region on brain MR-diffusion images (Figure 2). With all these MR findings, the mass was interpreted as a malignant tumor. However, considering that the existing malignant tumor might be metastatic, a contrast-enhanced CT scan of the thorax, abdomen, and pelvis revealed no tumor focus. Venous blood samples obtained from the patient showed that carcinoembryonic antigen level was 0.5 ng/ml, Ca 19-9 level was 17 U/ml (normal range 0-39 U/ml), Ca 15-3 was 5 U/ml (normal range 0-28.5 U/ml), Ca 125 level was 19 U/ml (normal range 0-35 U/ml), alpha-fetoprotein level was 2. 3 ng/ml (normal range 0-7 ng/ml) and beta-HCG level was <0.1 mlU/ml (normal range 0-10 mlU/ml).

With the above-mentioned results, the tumor was primarily considered a glial tumor, and the patient underwent surgery under neuro-navigation. Through the right occipital craniotomy, the localization of the tumor was reached, and as soon as the tumor capsule was penetrated, yellow-green, thick, odorless purulent discharge was seen draining from the mass, and samples taken from the discharge were sent to the relevant departments for urgent smear, culture, and pathological examination. After the fluid content of the tumor was completely drained, the tumor capsule and surrounding gliotic tissues were completely excised. Gram-positive diplococci were detected in the emergency smear preparations and "*Streptococcus porcinus*" growth was detected in the subsequent culture slides. Cytologic examination showed negative cytology for malignancy. Pathological examination revealed inflammatory necrosis, gliosis, foci of necrosis surrounded by increased vascularization in glial tissue, reactive dendroglial proliferation and lymphatic infiltration, and inflammatory cell infiltration rich in polymorphonuclear leukocytes on necrobiotic background which may be compatible with abscess content. With these findings, the Infectious diseases department started a vancomycin and meropenem regimen, intravenously.

The patient underwent control contrast-enhanced brain MR imaging in the early postoperative period and a heterogeneous contrast-enhancing parenchymal area of 23 millimeters in diameter was found in the right occipital region with edema around it. Venous blood samples taken one week after the operation showed a leukocyte count of 13530/µl, CRP level of 0.72 mg/L, procalcitonin level of 0.026 ng/ml, and vancomycin treatment was discontinued by the Infectious diseases department.

The ophthalmology department examined the patient in the second month after surgery and the visual field was found to be normal as a result of the confrontation test. In venous blood samples taken during this period, leukocyte count was 6960 uL, CRP level was 0.4 mg/L, and procalcitonin level was 0.032 ng/ml. Contrast-enhanced brain MRI performed four months after surgery revealed a 10x7 millimeter area of diffusion restriction in the right occipital lobe. In venous blood samples

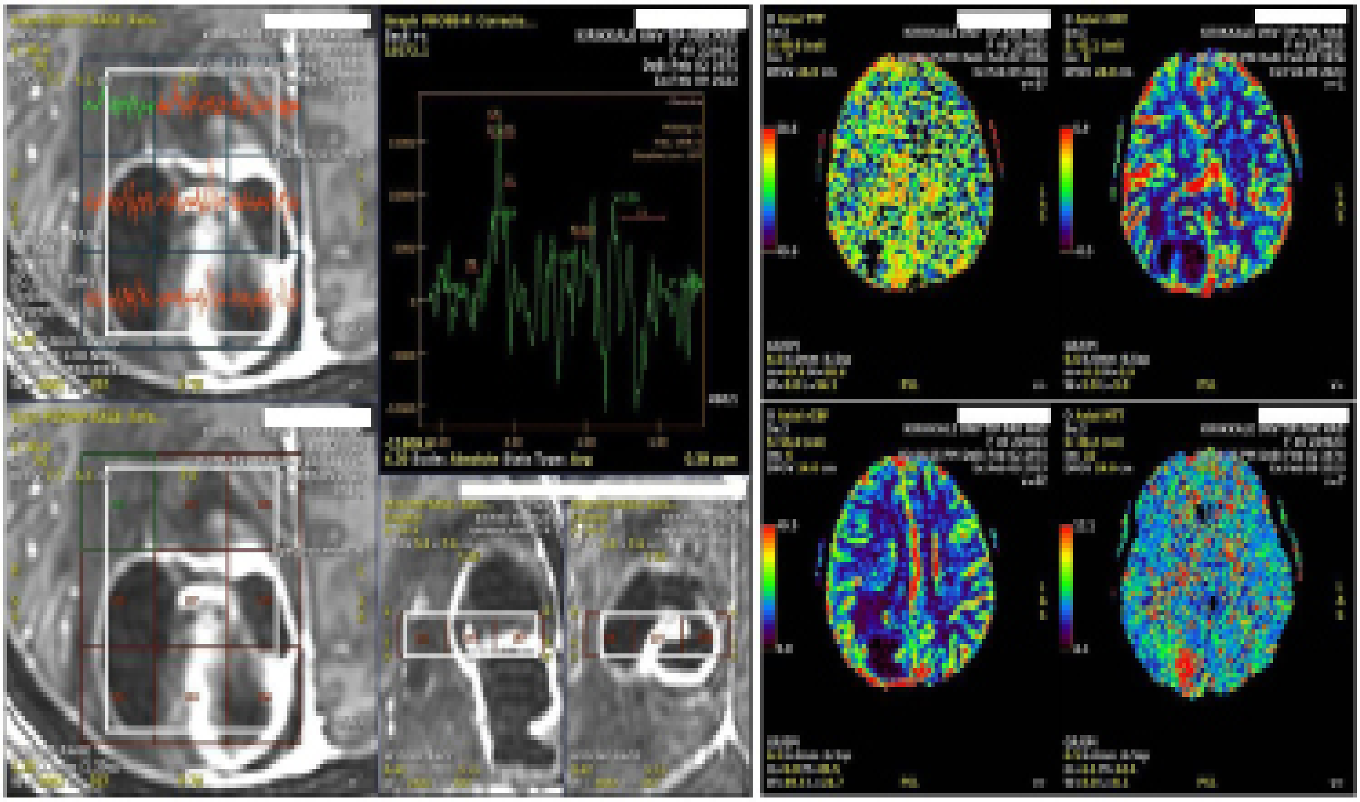

Figure 2. In the MR spectroscopy images (left side of the figure), significant choline-creatinine and choline-NAA peaks in favor of malignancy are seen in the right occipital lobe. In the MR perfusion images (right side of the figure), TTP, CBV, CBF, and MTT values that show changes in favor of malignancy are observed in the same region.

obtained simultaneously, leukocyte count was 6540 ul, CRP level was 0.86 mg/L, and procalcitonin level was <0.020 ng/ml. The Infectious Diseases Department terminated intravenous meropenem treatment at the end of the fifth month due to the normalization of blood biochemistry values and marked improvement in brain MR images. Ten months after the operation, contrast-enhanced brain MR images showed a sequel encephalomalacia area in the periventricular region of the right occipital lobe extending towards the parietal lobe (Figure 3).

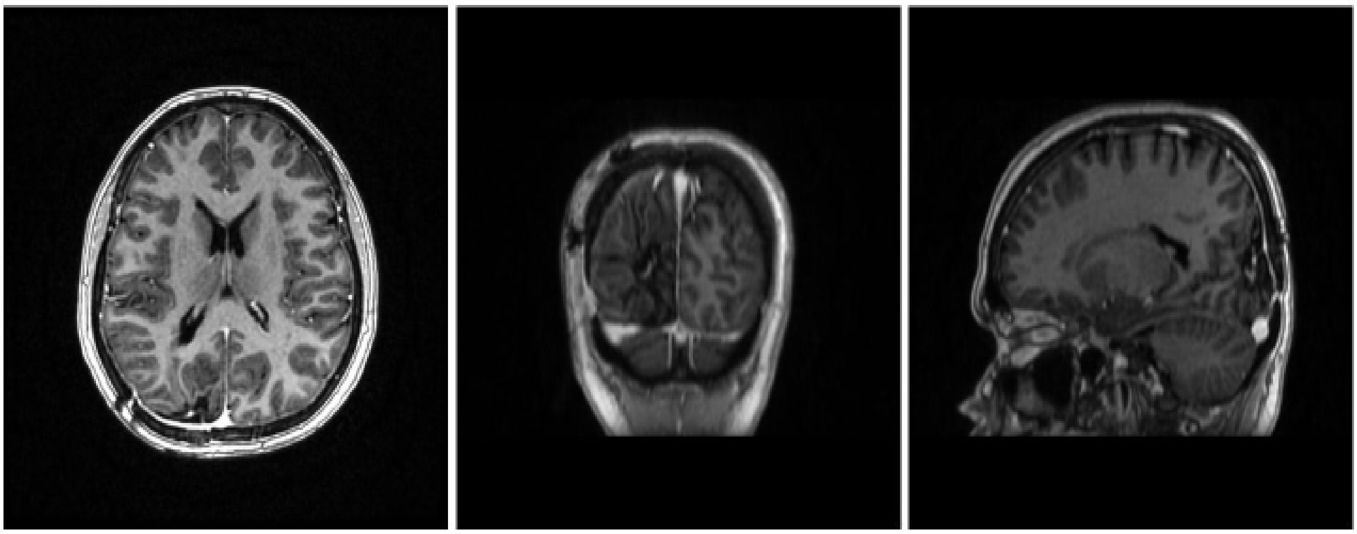

Figure 3. Contrast-enhanced MR images taken at the 10th postoperative month show encephalomalacia changes and peripheral gliosis in a location corresponding to the right posterior cerebral artery irrigation area.

DISCUSSION

Brain tumors are mainly divided into primary brain tumors and metastases. Another group of space-occupying lesions that may be similar to these tumors are brain abscesses. Brain abscesses are intracranial masses with focal collections and suppurative processes in the brain parenchyma that occur as a complication of various infections such as bacteria, mycobacteria, fungi or parasites, trauma, or surgical interventions.[1,2] It has been suggested in the literature that it would be appropriate to analyze these masses with diffusion MR sequences (DWI), perfusion-weighted MR imaging (DSCE-PWI), and MR-spectroscopy to characterize this lesion, since the appearance on conventional MR images is unclear in the differentiation of intracranial abscess from tumor or metastasis.[5] In a study, it has been reported that

MR-spectroscopy had moderate diagnostic performance in distinguishing high-grade gliomas from low-grade gliomas. The choline/NAA ratio obtained in this study showed higher sensitivity and specificity than the choline/creatinine and NAA/Creatinine ratios and should be combined with other advanced imaging techniques such as MR-diffusion and MR-perfusion to improve diagnostic accuracy.[6] On the other hand, a meta-analysis study reported that the diagnostic value of MR-spectroscopy in differentiating glial tumors from metastatic brain tumors was average and that the Choline/ NAA ratio should be used to increase this diagnostic value.[7] In addition, it has been reported that the ADC values and ADC ratios of MR-perfusion examination can also help differentiate metastases from high-grade gliomas, but it is not very successful in differentiating high-grade gliomas from lymphomas and lymphomas from metastases.[8]

In addition, serum tumor-specific biochemical markers may also be diagnostic aids, especially in the differentiation of metastatic brain tumors and other intracranial space-occupying lesions. However, it is also known that serum levels of these markers may be elevated in most benign and malignant diseases. Similarly, these markers alone are not sufficient to make an early diagnosis of most diseases and even to detect recurrence or advanced disease, therefore, it is recommended that they should be used together with other evaluation methods in clinical practice.[4]

Based on the physical and neurological examination performed when the patient was admitted to the emergency department, it was thought that the patient might have an intracranial lesion (such as a stroke, tumor, etc.), and a brain CT was performed. The brain CT image showed a mass with edematous surroundings. Contrast-enhanced brain MR and MR-spectroscopy were performed for the differential diagnosis of the intracranial mass. Upon detection of choline/ NAA peaks, this mass was thought to be a malignant tumor, since decreased choline, creatine, and NAA levels are expected in non-neoplastic lesions such as brain infarction and brain abscess.5 In addition, brain MRI-diffusion images showed a patchy diffusion restriction in the localization of the tumor, and brain MR-perfusion images showed that TTP, CBV, CBF, and MTT values showed changes in favor of malignancy in the localization of the tumor and this tumor was thought to be a malignant intracranial tumor. Contrast-enhanced CT scan of the thorax, abdomen, and pelvis was performed to determine whether the intracranial tumor was a primary brain tumor or a metastasis. No other foci were detected in the scans. Since the serum tumor markers were also negative, a primary malignant brain tumor (most likely a glial tumor) was considered.

Contrary to all these considerations, when the capsule of the mass was penetrated during the surgical intervention, a yellow-green colored, thick, odorless purulent discharge was seen coming out of the mass and all pathological examinations revealed that the mass was a brain abscess. In conclusion, although the patient's clinical presentation and detailed radiological imaging studies suggested a primary malignant brain tumor, the patient was diagnosed with a brain abscess as a result of pathological examinations. Considering the etiology of brain abscess, it was concluded that untreated tooth decay may be the cause of brain abscess, although no obvious focus of infection was detected in the patient's body.

CONCLUSION

As seen in this patient, radiologic imaging may sometimes not be sufficient to make the correct diagnosis and may lead to different diagnoses. Therefore, it was thought that it would be appropriate to keep in mind the margin of error of the examinations when making a preliminary diagnosis in patients with brain tumors and to take precautions by keeping in mind the less probable preliminary diagnoses as well as the probable preliminary diagnoses.

ETHICAL DECLARATIONS

Informed Consent

The patient signed and free and informed consent form.

Referee Evaluation Process

Externally peer-reviewed.

Conflict of Interest Statement

The authors have no conflicts of interest to declare.

Financial Disclosure

The authors declared that this study has received no financial support.

Author Contributions

All of the authors declare that they have all participated in the design, execution, and analysis of the paper, and that they have approved the final version.

REFERENCES

1. Oyar O. Magnetik rezonans görüntüleme (MRG)' nin klinik uygulamaları ve endikasyonları. *Harran Üniversitesi Tıp Fakültesi Derg.* 2008;5(2):31-40.
2. Arı A, Hanbay D. Tumor detection in MR images of regional convolutional neural networks. *Am J Pharm Educ. and Architecture of Gazi University.* 2019;34(3):1395-1408
3. Esen OS, Bozkurt M, Adıbelli ZH, Aykut E, Canverenler S. Proton MR spektroskopinin beyin tümörlerinde tanısal değeri. *Tepecik Eğit Hast Derg.* 2014;24(2)93-98.
4. Dumlu E. Tümör belirteçlerinin klinik kullanımı; ne zaman isteyelim? *Türk Tıp Dergisi.* 2015:7(1):124-127.
5. De Simone M, Brogna B, Sessa G, Oliva G, Guida B, Magliulo M. Valuable contribution of magnetic resonance spectroscopy in differentiation of brain abscess from glioma. *Infect Dis.* 2017;49(11-12):871-873.
6. Wang Q, Zhang H, Zhang J, et al. The diagnostic performance of magnetic resonance spectroscopy in differentiating high-from low-grade gliomas: a systematic review and meta-analysis. *Eur Radiol.* 2016;26(8):2670-2684.
7. Wang Q, Zhang J, Xu W, Chen X, Zhang J, Xu B. Role of magnetic resonance spectroscopy to differentiate high-grade gliomas from metastases. *Tumour Biol.* 2017;39(6):1010428317710030.
8. Server A, Kulle B, Maehlen J, et al. Quantitative apparent diffusion coefficients in the characterization of brain tumors and associated peritumoral edema. *Acta Radiol.* 2009;50(6):682-689.